New Tools For Texture Research

Jerzy Szpunar and Hualong Li
McGill Unversity
Montreal, Canada

For demonstration of texture analysis software, go to

www.resmat.com

- F. Czerwinski, D. Li, K. Lee, P. Blandford,
- Hualong Li, Zhang Li, D. Hinz, R. Rajmohan. V. Gertzman, A. Zhilyaev

Acknowledgments

Why Study Texture in Films?

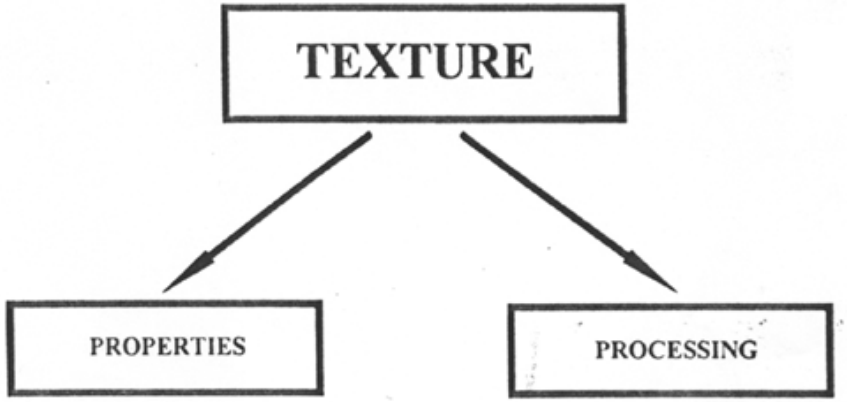

PROPERTIES AND APPLICATIONS

- semiconductor films
- insulating and conductive films
- films for magnetic recording
- magnetic recording heads
- optical recording
- superconductive films
- magnetic multilayers
- diffusional, protective and thermal coatings
- tribology of films and coatings
- diamond films

PROCESSING

- physical vapour deposition
- chemical vapour deposition
- sol-gel
- electroplating
- annealing
- laser modification
- ion implantation

tmquen48.021

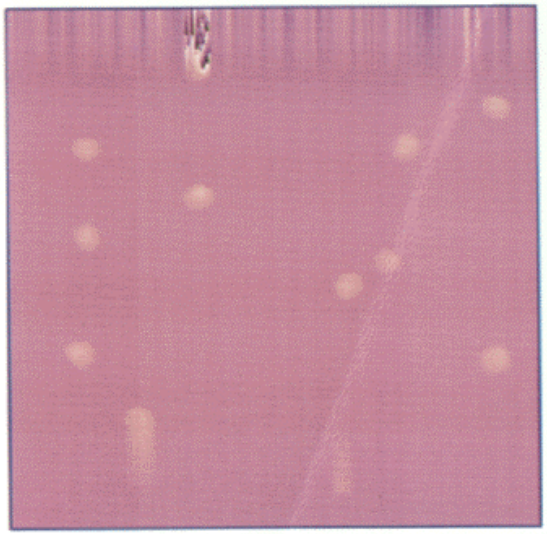

tmquen44.001

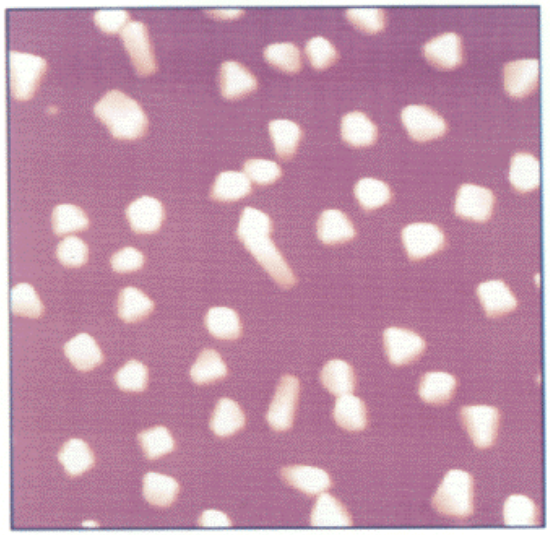

tmquen49.001

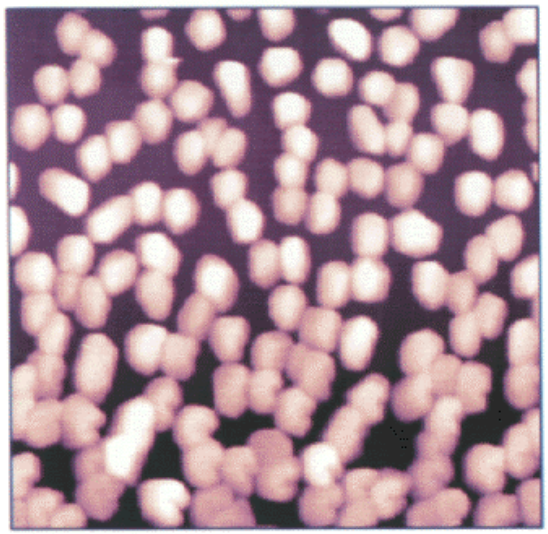

tmquen46.001

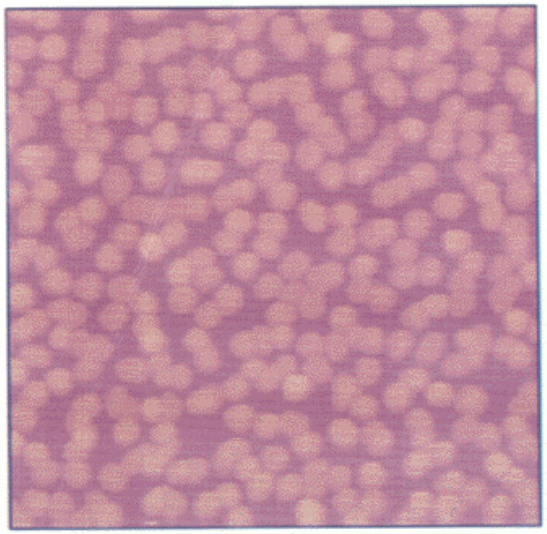

tmquen51.002

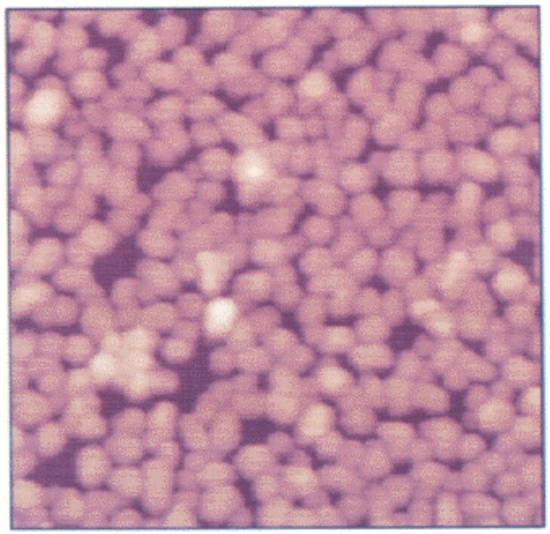

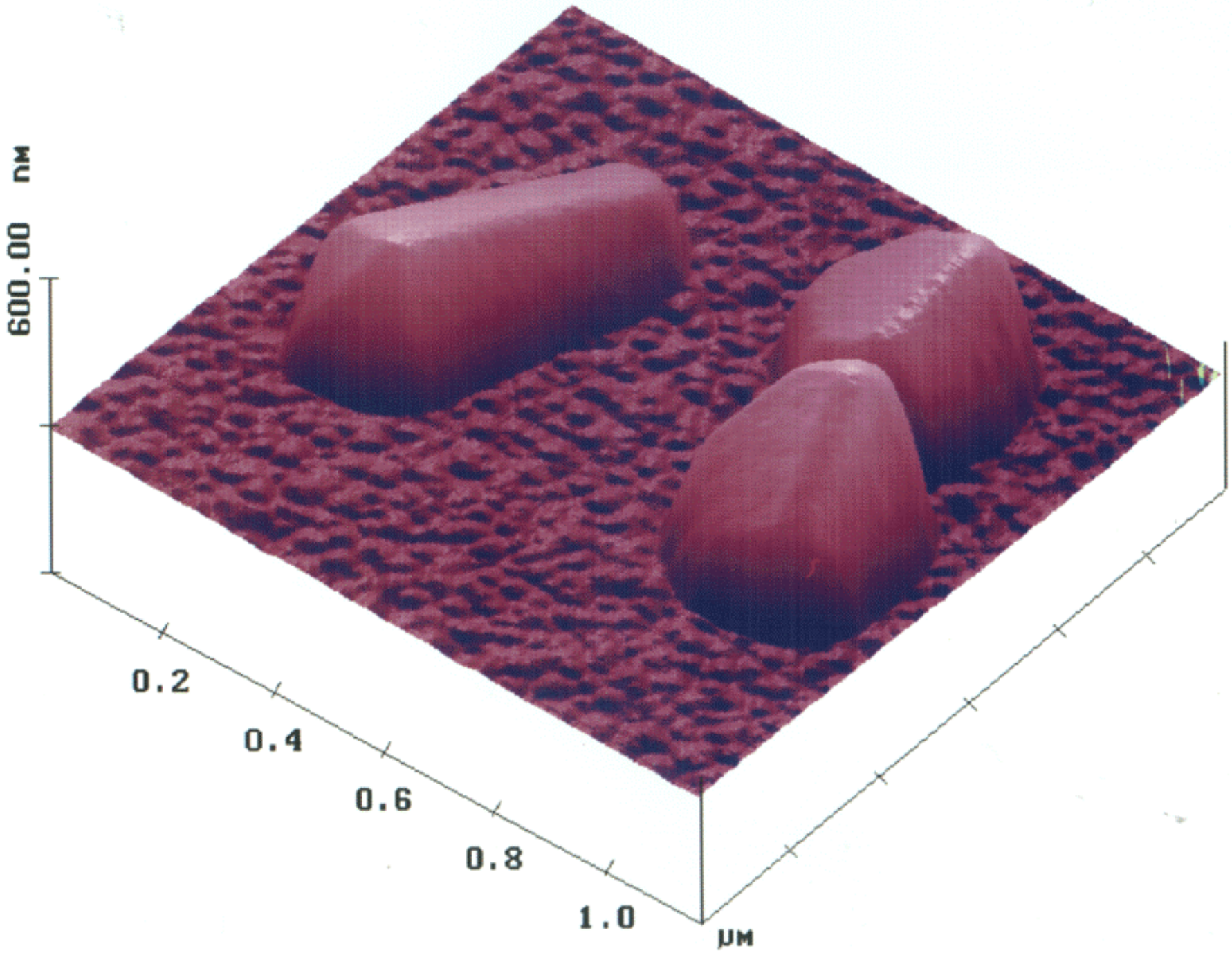
600.00 nm
0.2
0.4
0.6
0.8
1.0
µm

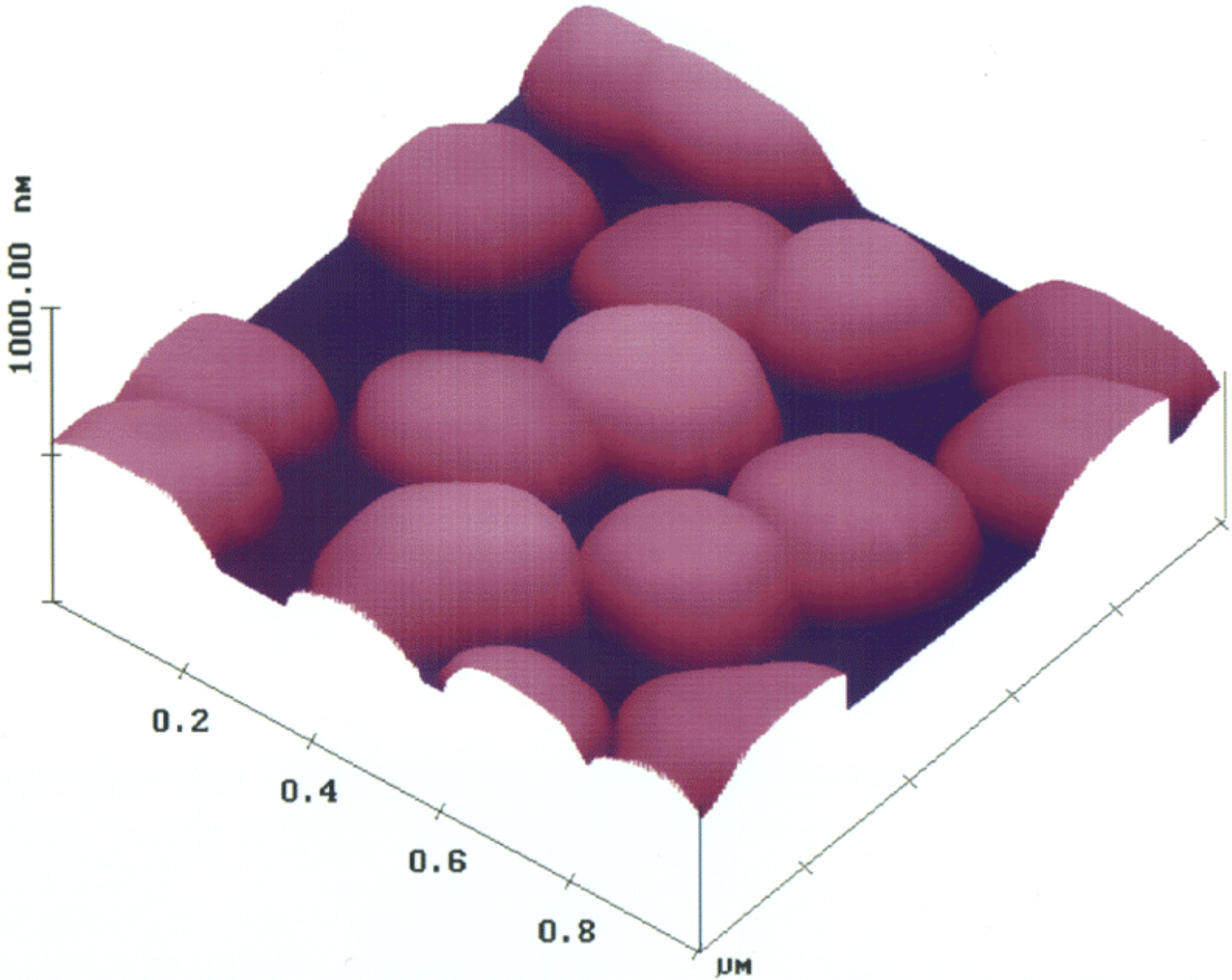
1000.00 nm
0.2
0.4
0.6
0.8
µm

TEXTURE MEASUREMENTS

- GRAZING INCIDENCE GEOMETRY

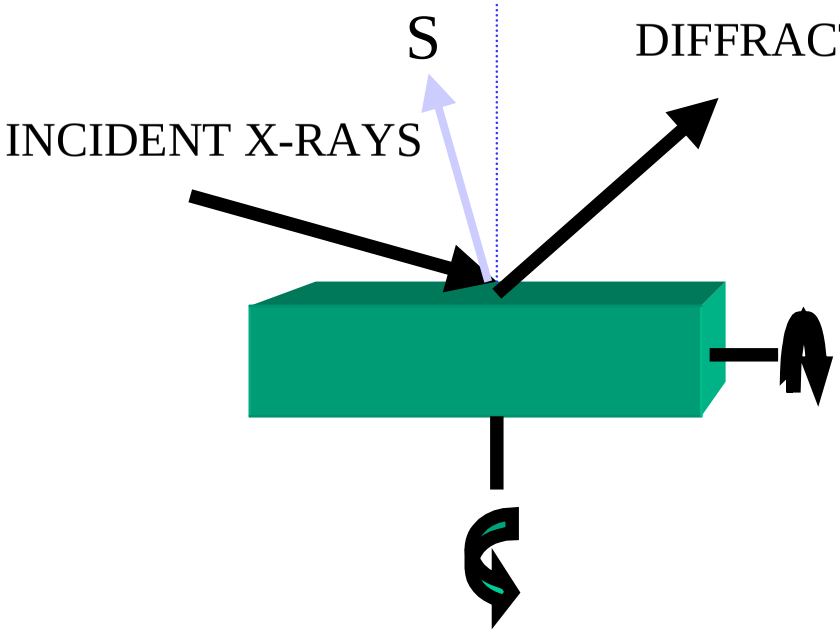

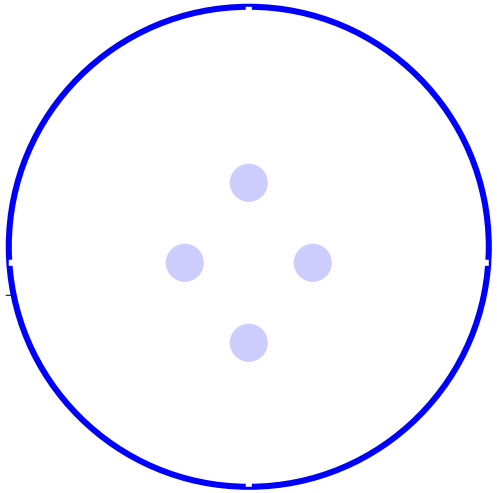

POLE FIGURE

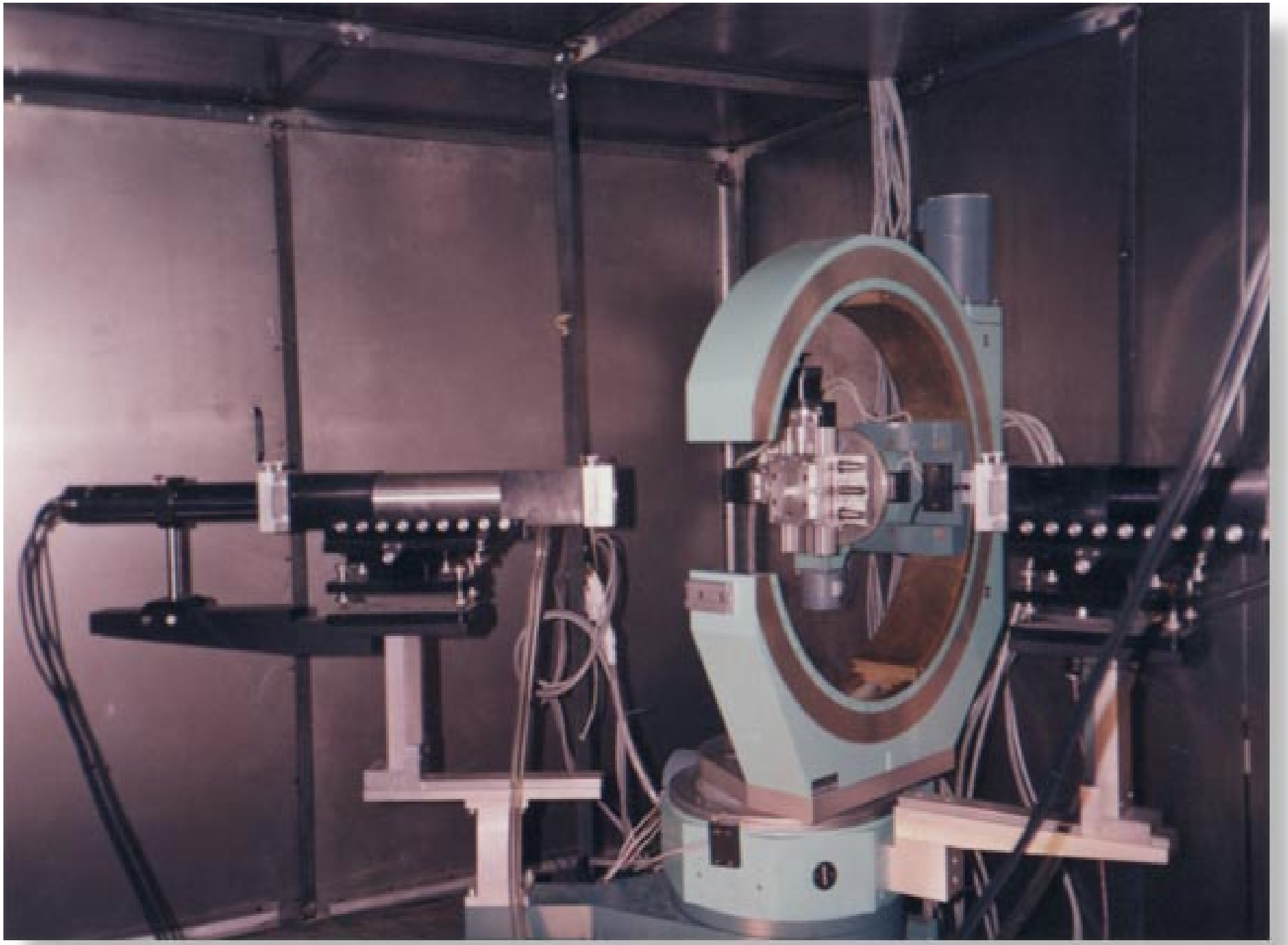

Photographs of the laboratory facility built to test methods for on-line texture analysis

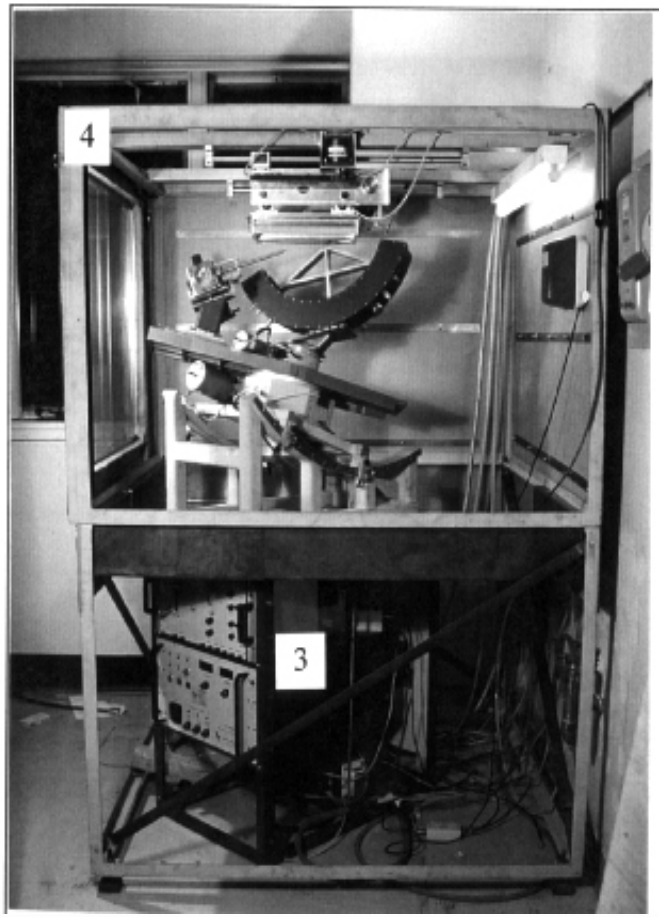

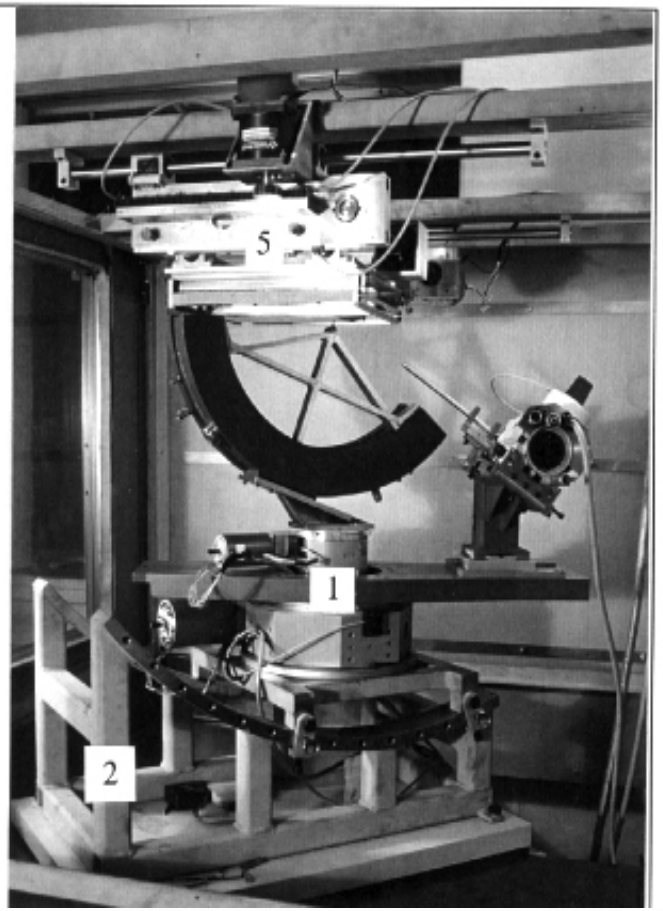


TEXTURE
Co-Cr FILMS FOR
MAGNETIC
RECORDING MEDIA

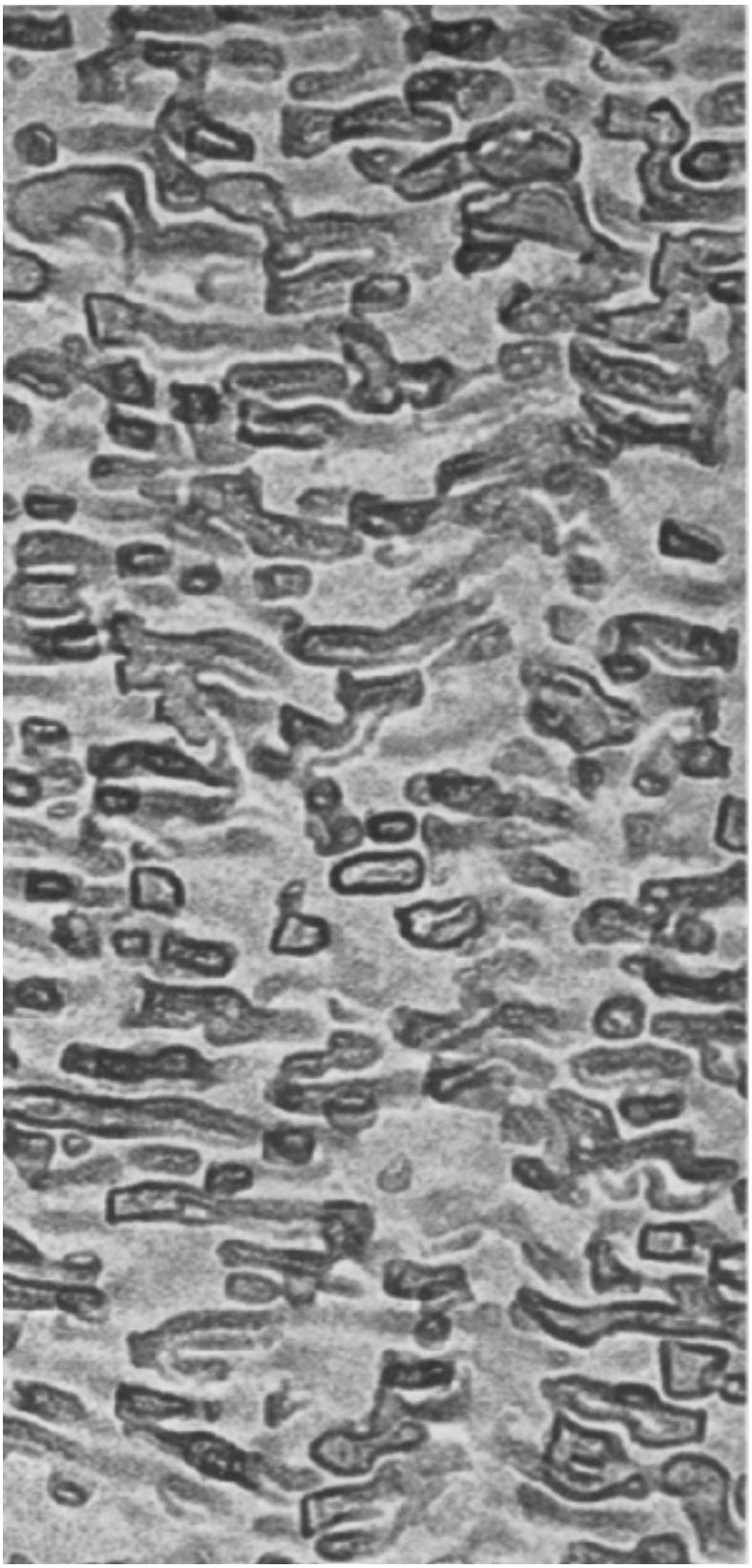

Results

THICKNESS:	**(5 - 1000) nm**
SUBSTRATE:	**(A) $Ge/SiO_2/Si$**
METHOD:	**SPUTTERING**
COMPOSITION:	**$Co_{81}Cr_{19}$**

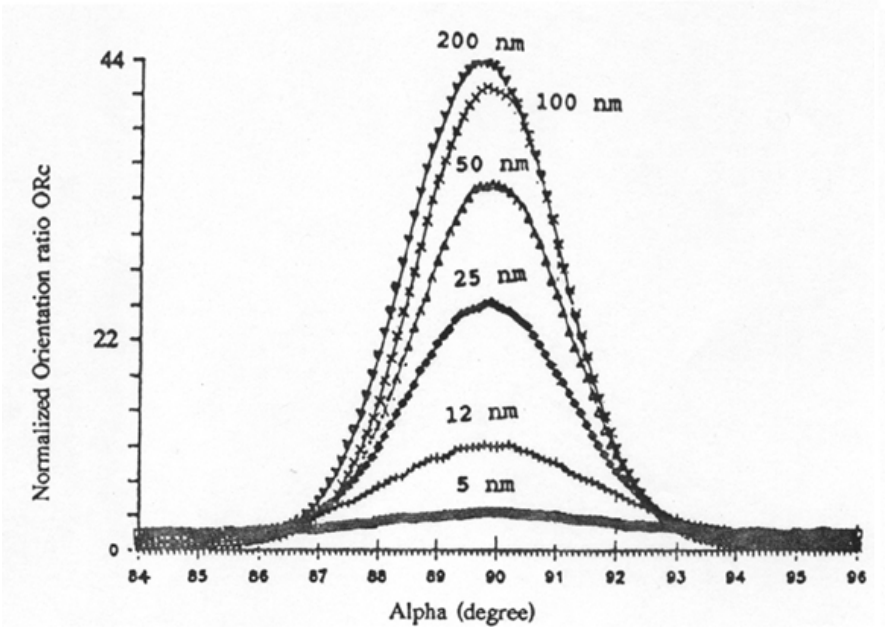

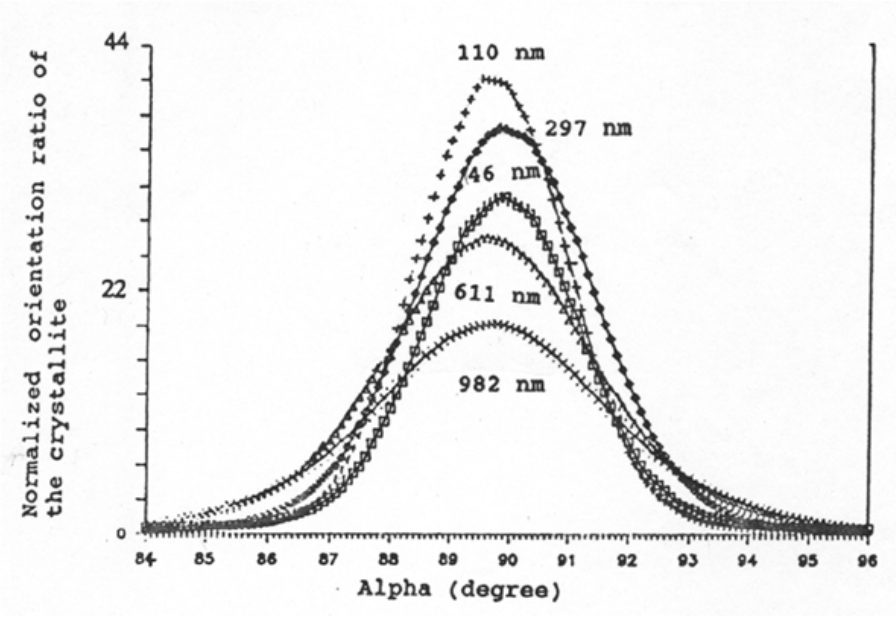

Model of Correlation Between Texture and Anisotropy of Magnetic Properties

- Uniaxial magnetic anisotropy of grains
- Unisome rotation of magnetization of particles towards the direction of the magnetic field
- Texture described by

$$P(\alpha) = \sum_{l=0}^{L} a_l^{\nu} k_l^{\nu}(\alpha)$$

The Measured and the Calculated $H_{c\perp}$ (With Magnetostatic Interaction Between Columnar Grains)

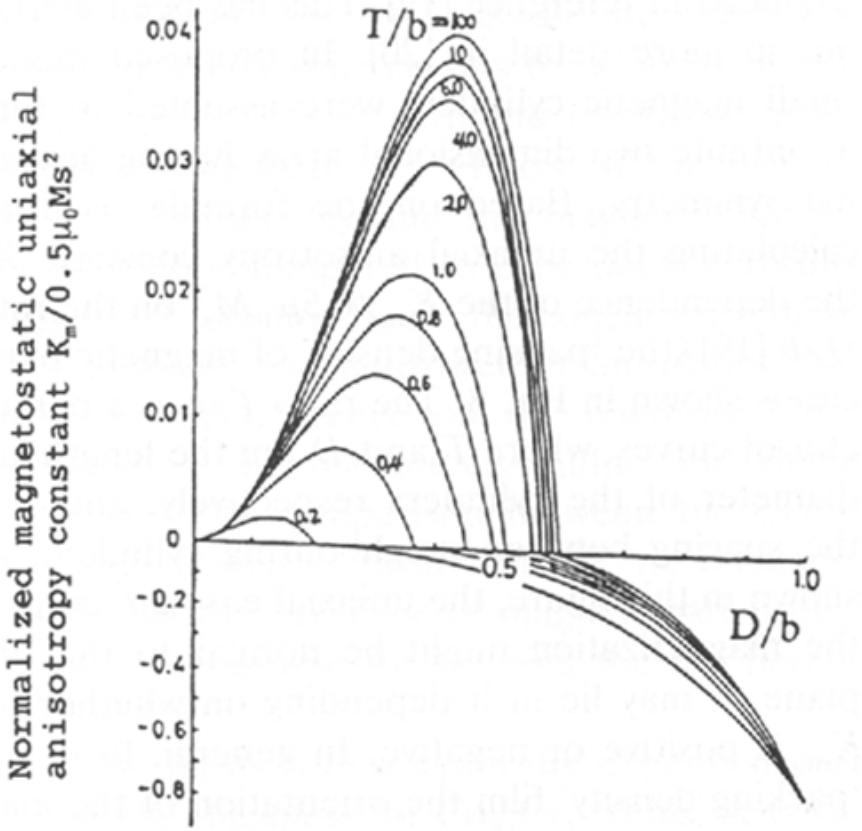

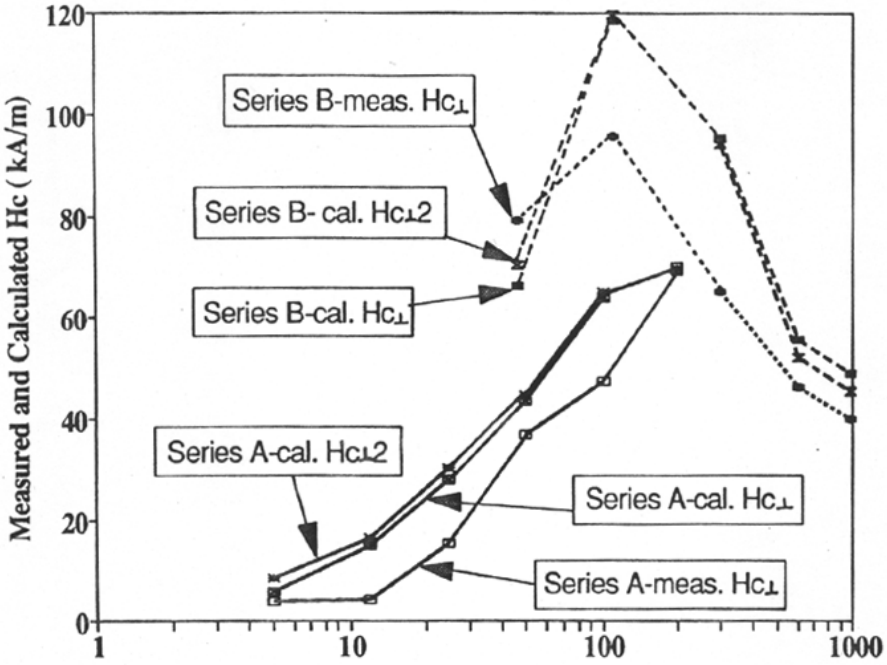

CONCLUSIONS

- TEXTURE PLAYS AN IMPORTANT ROLE IN OPTMIZING THE PROPERTIES OF Co-Cr FILMS
- MAGNETIC PROPERTIES CAN BE CORRELATED TO ORIENTATION AND SHAPE OF GRAINS
- TEXTURE STRENGTH DEPENDS ON THE FILM THICKNESS


Texture in iron
oxides

Preliminary Results

Anisotropy of the growth of iron oxides

The relative intensity ratio of magnetite and hematite peaks as a function of temperature.

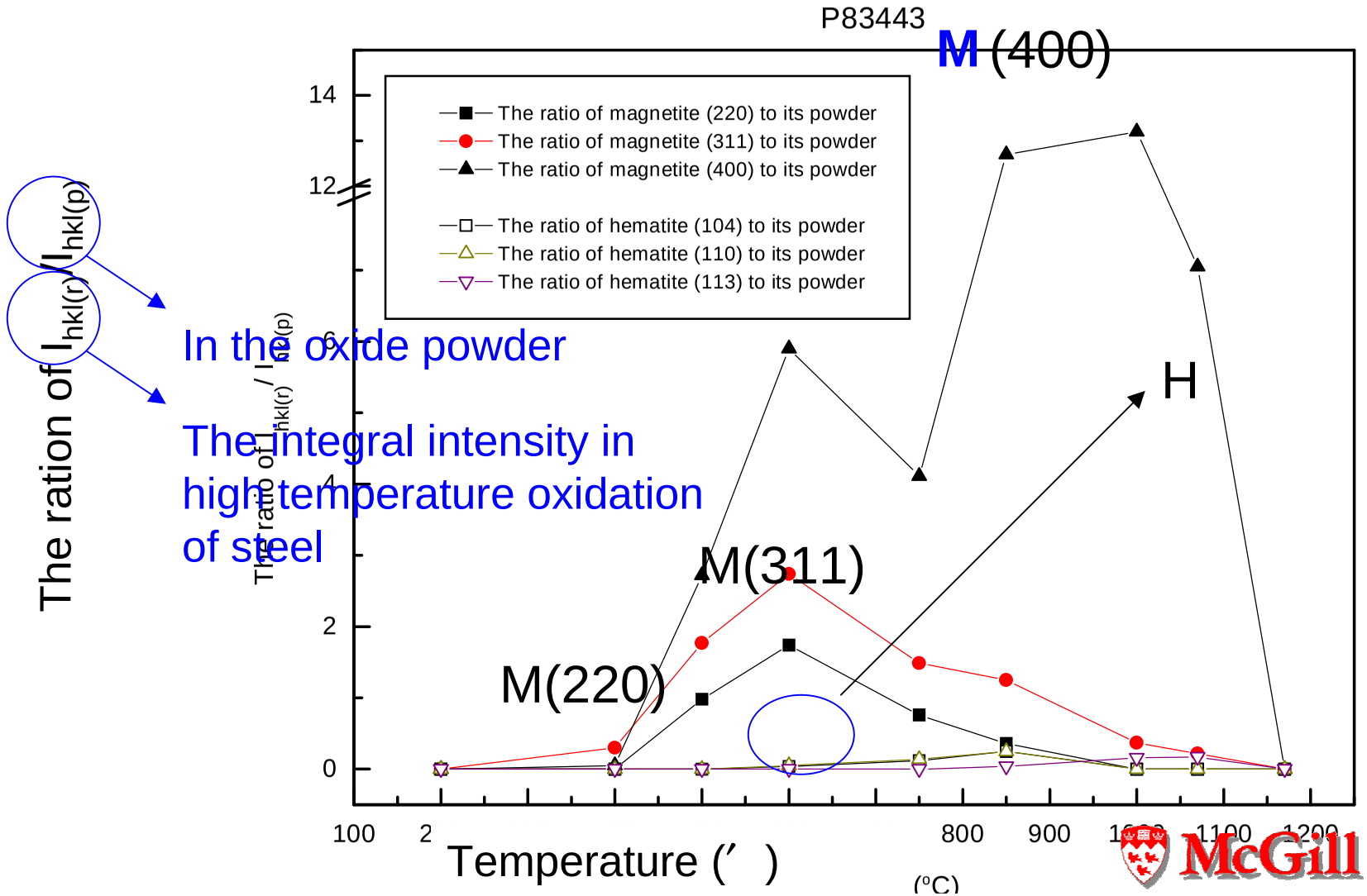

McGill

Preliminary Results

Anisotropy of oxide growth and texture

Free surface

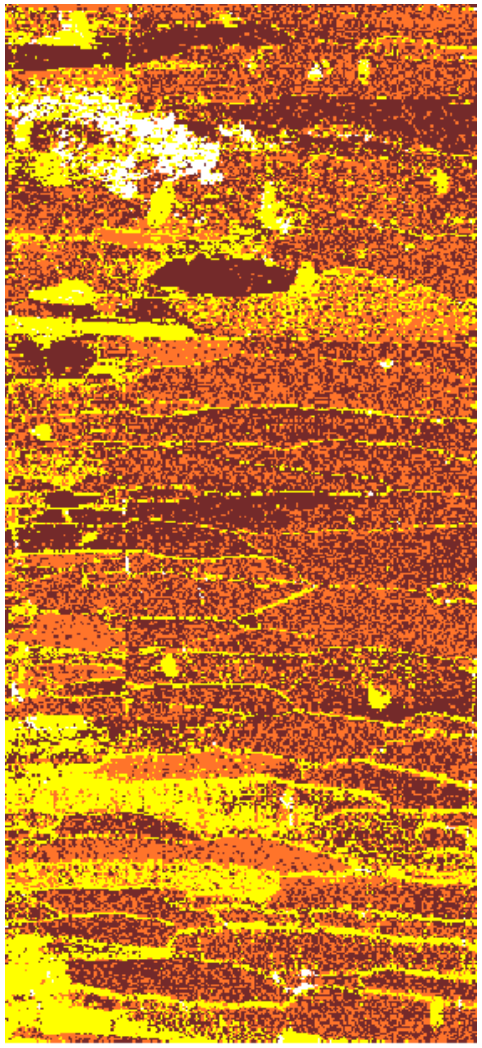

22.50 µm = 45 steps

Fe

OIM

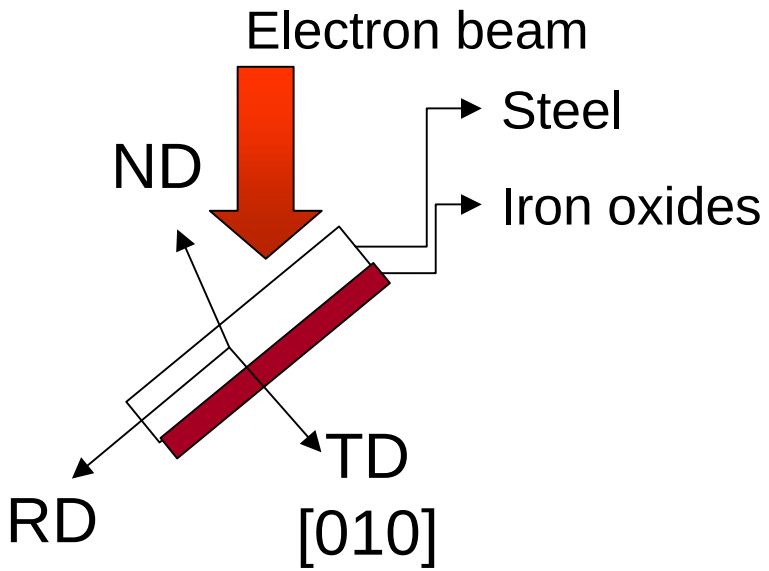

Wüstite

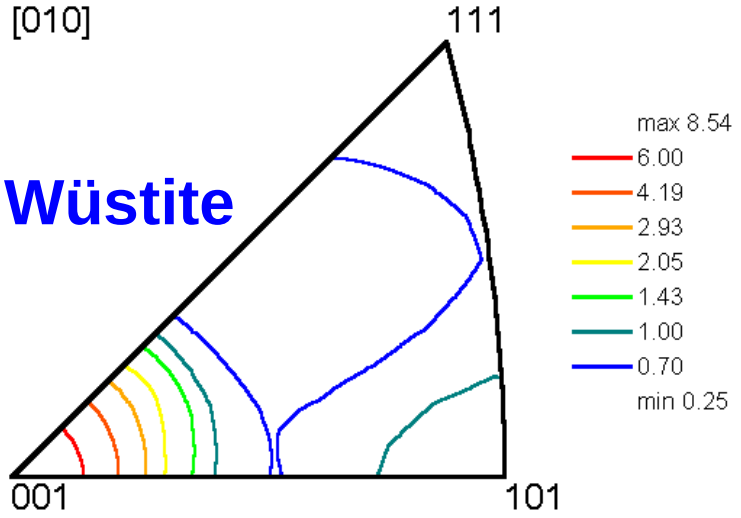

McGill

CONCLUSIONS

- WUSTITE, MAGNETITE AND HEMATITE ARE TEXTURED
- TEMPERATURE OF OXIDATION PLAYS AN IMPORTANT ROLE IN CONTROLLING THE STRENGTH AND TYPE OF TEXTURE

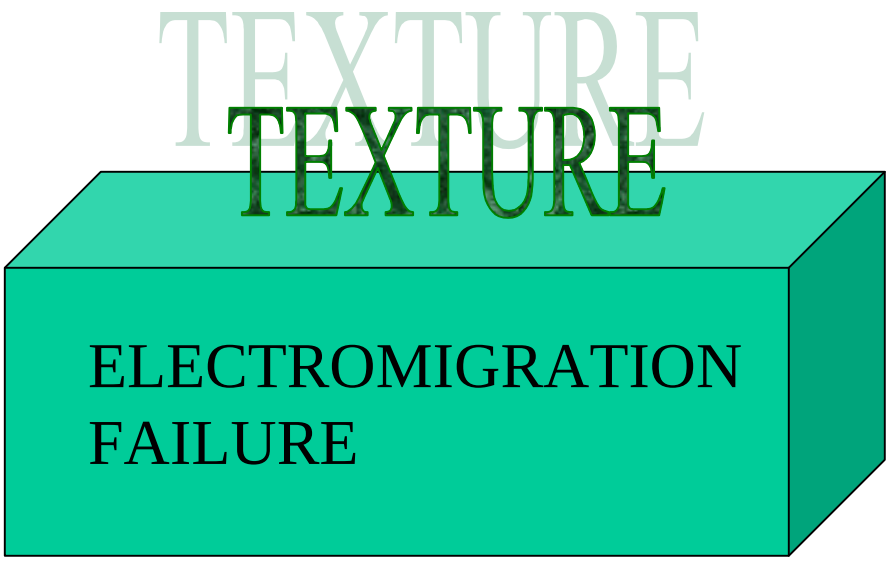
TEXTURE
TEXTURE
ELECTROMIGRATION
FAILURE

Typical Electromigration Failures

Figure IV.1.(a)

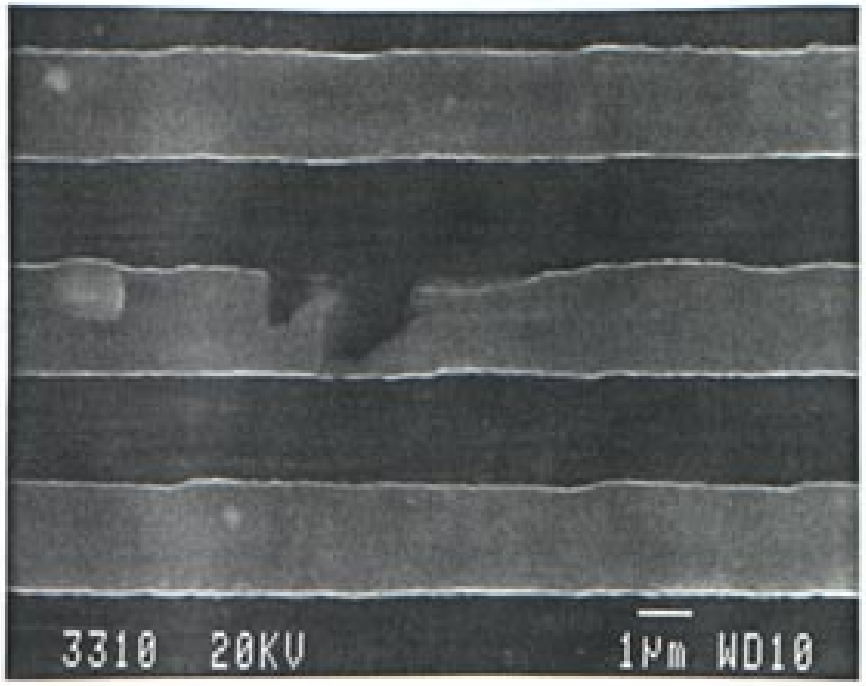

Figure IV.1.(b)

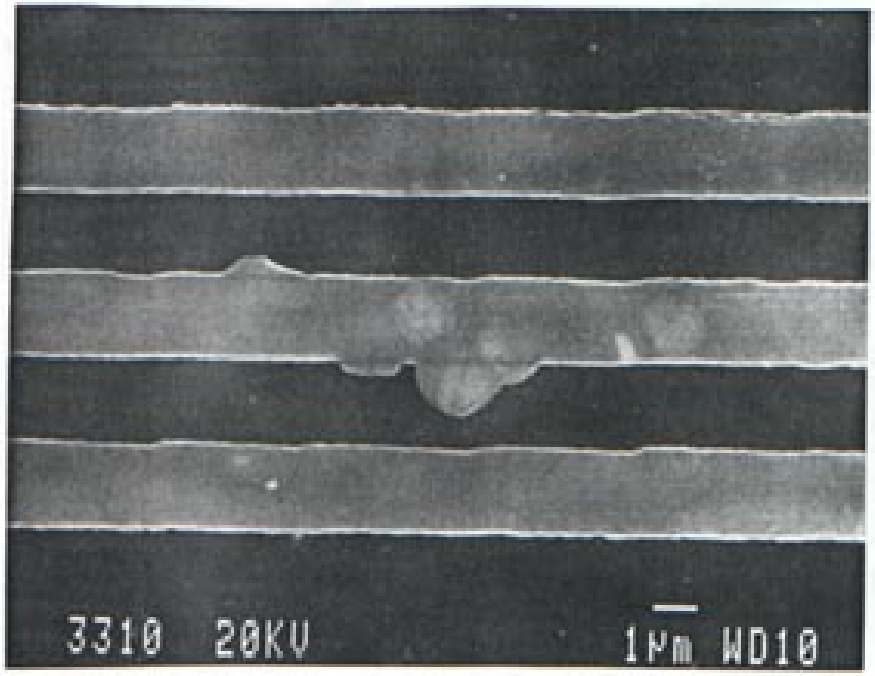

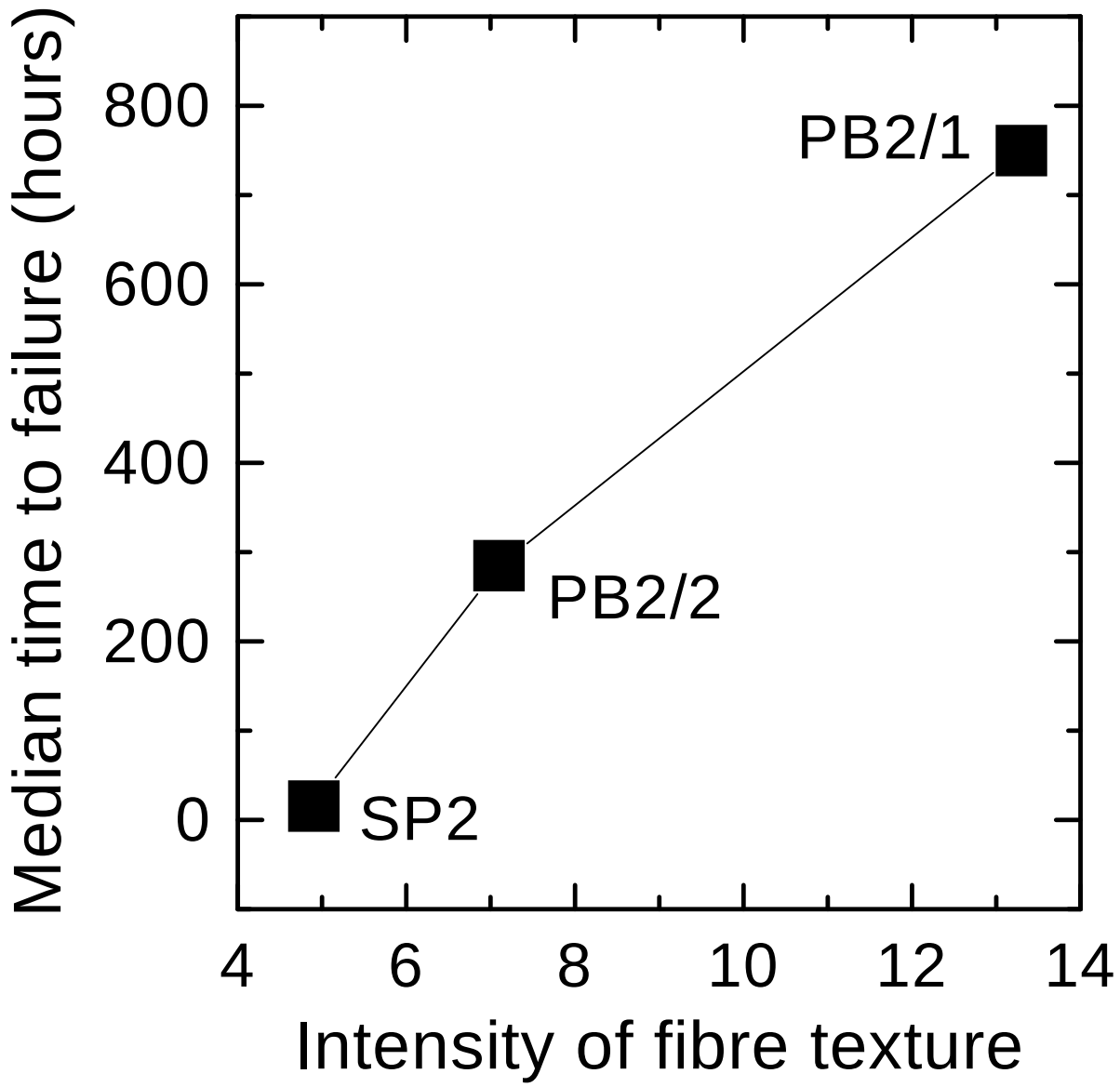
Median time to failure (hours)
800
600
400
200
0
PB2/1
PB2/2
SP2
4
6
8
10
12
14
Intensity of fibre texture

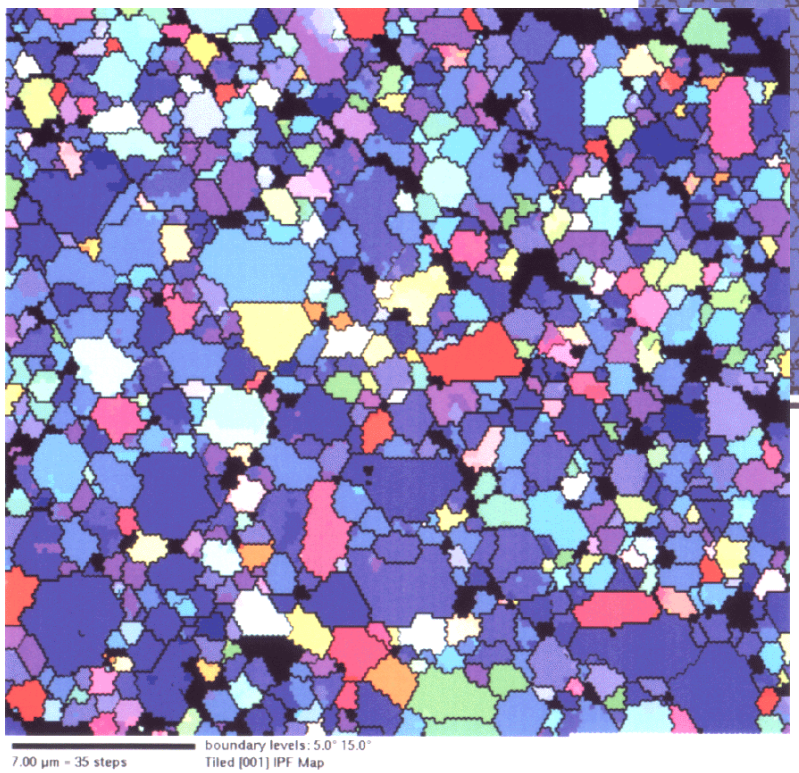
7.00 µm = 35 steps
boundary levels: 5.0° 15.0°
Tiled [001] IPF Map

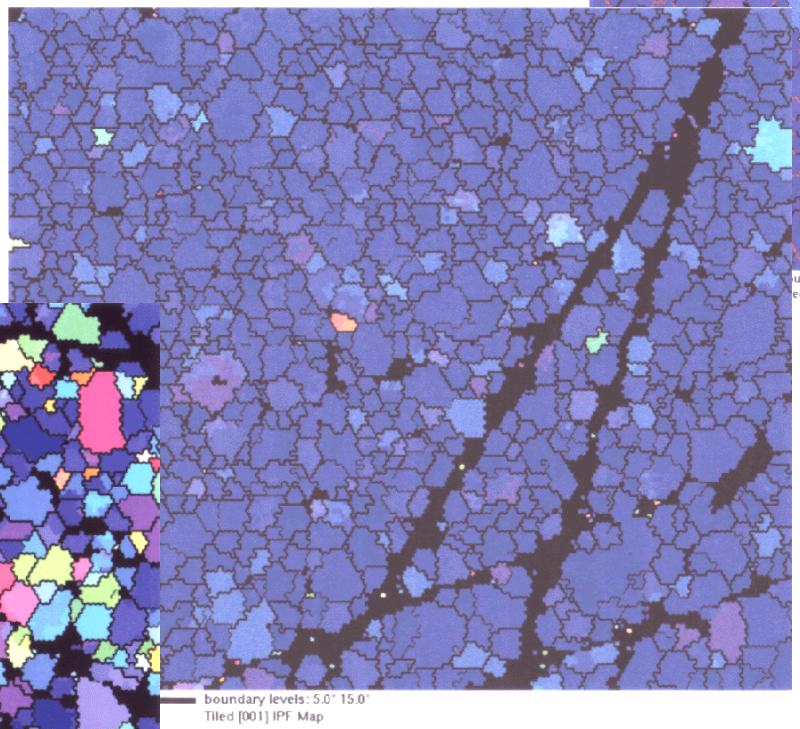
boundary levels: 5.0° 15.0°
Tiled [001] IPF Map

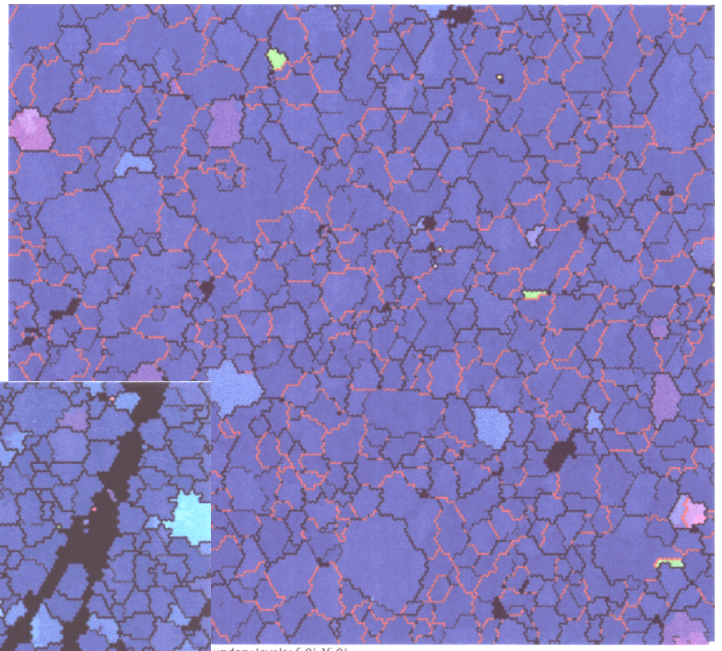
undary levels: 5.0° 15.0°
ed [001] IPF Map

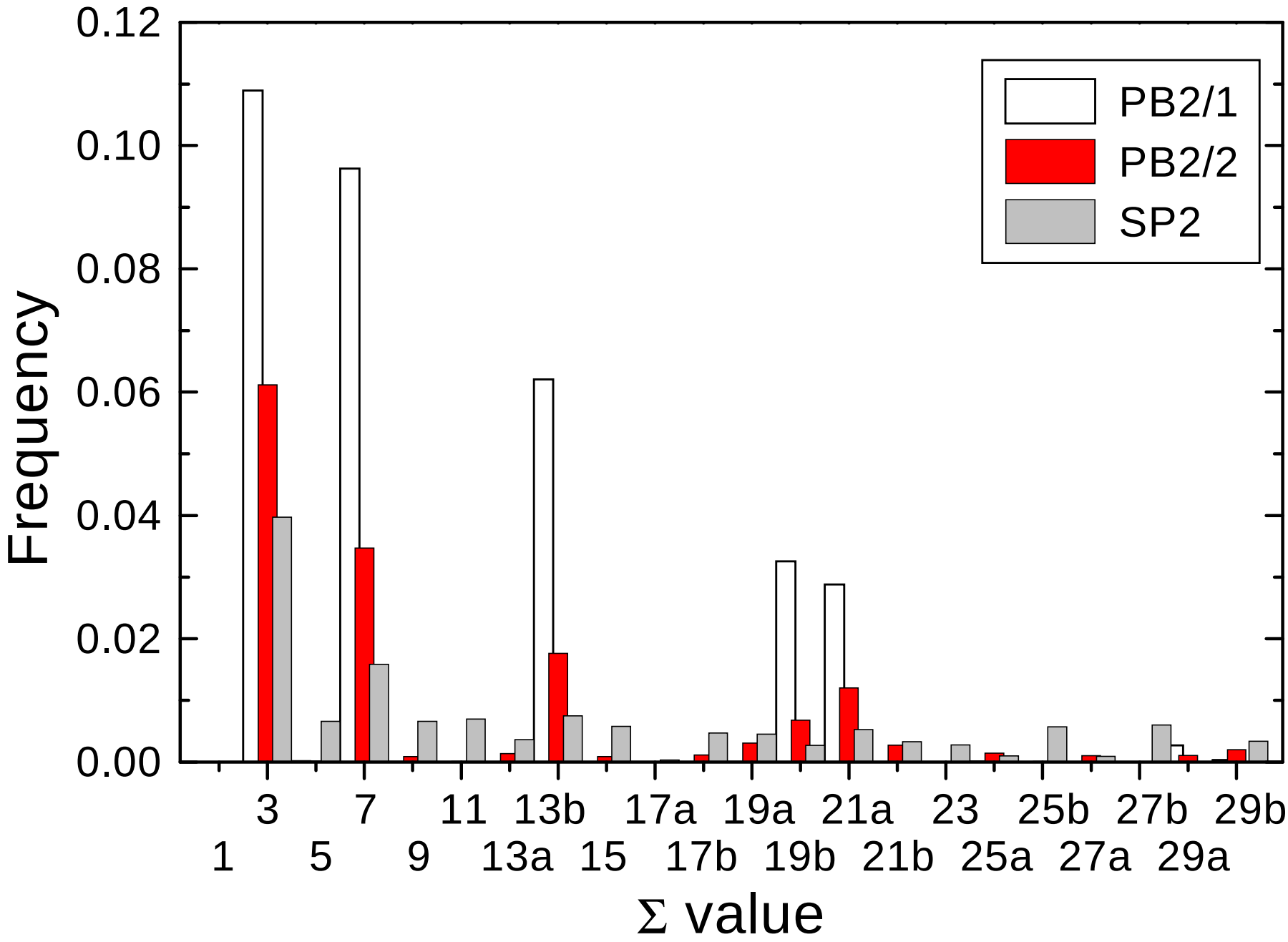
0.12
0.10
0.08
0.06
0.04
0.02
0.00
Frequency
PB2/1
PB2/2
SP2
1
3
5
7
9
11
13a
13b
15
17a
17b
19a
19b
21a
21b
23
25a
25b
27a
27b
29a
29b
Σ value

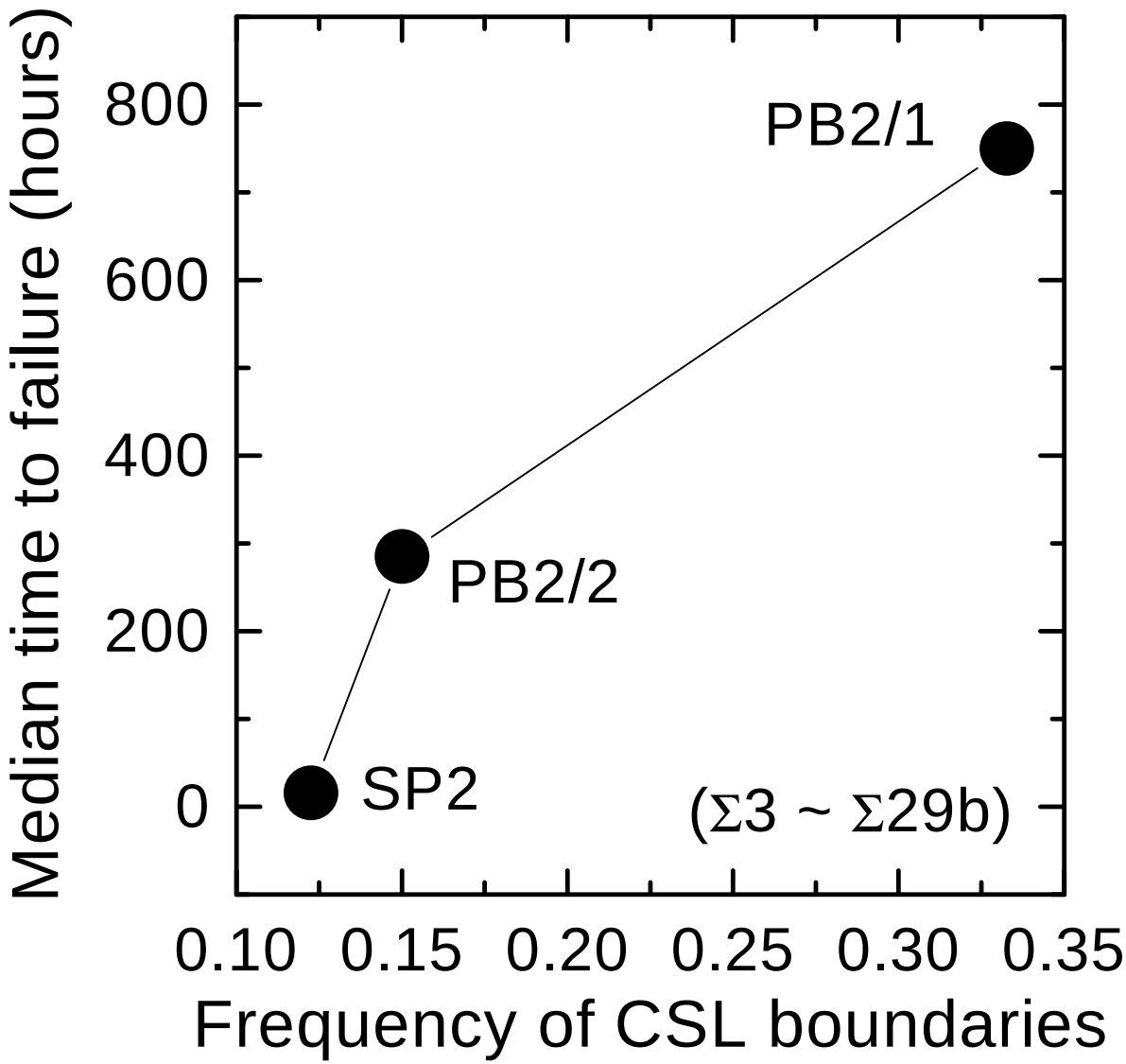
Median time to failure (hours)
800
600
400
200
0
PB2/1
PB2/2
SP2
(Σ3 ~ Σ29b)
0.10
0.15
0.20
0.25
0.30
0.35
Frequency of CSL boundaries

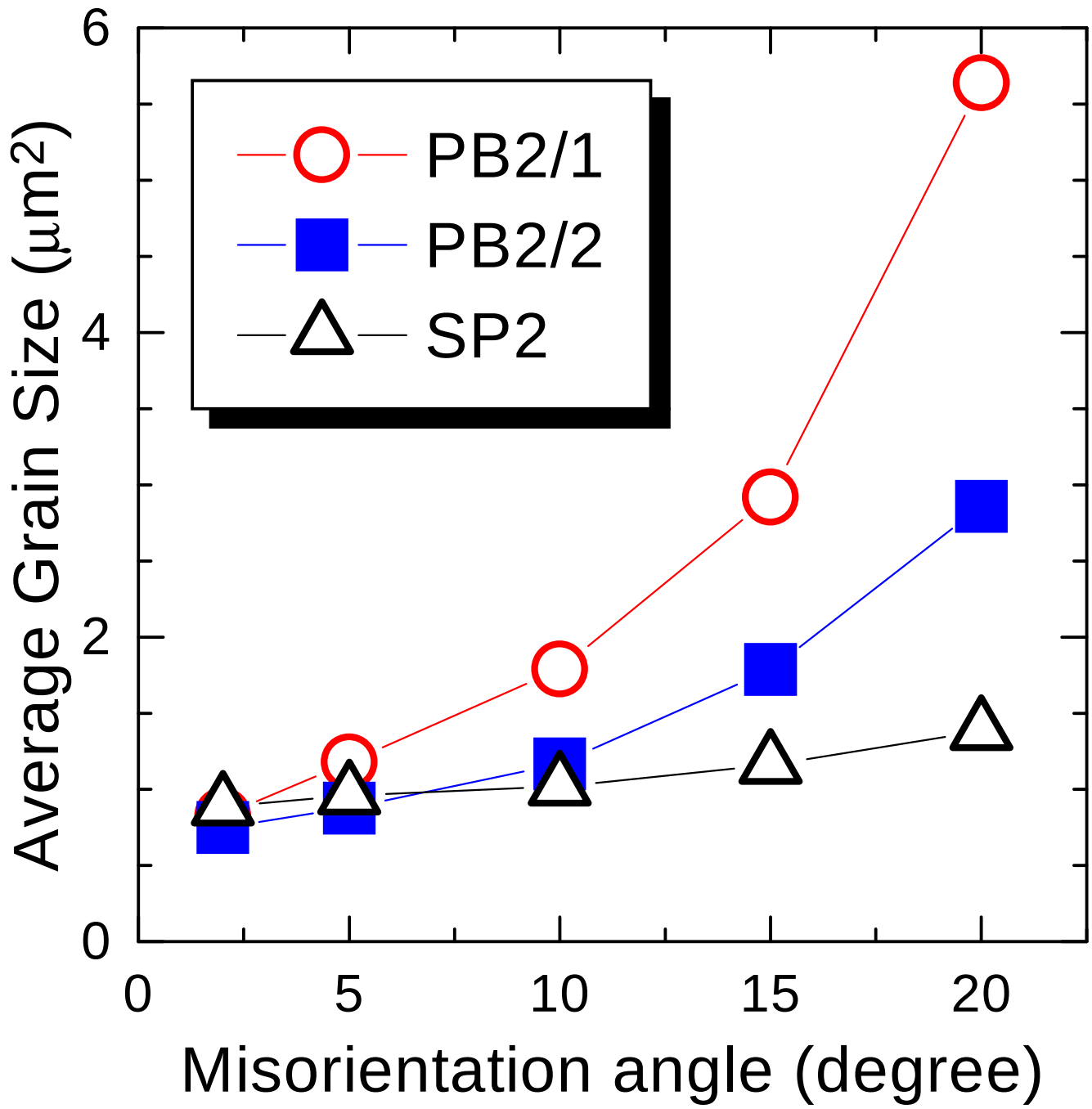
PB2/1
PB2/2
SP2
Average Grain Size (μm²)
Misorientation angle (degree)
0
2
4
6
0
5
10
15
20

Message

- Texture engineering can be used to improve the life time of electronic interconnects.
- Better understanding of a role of texture in failure of electronic multi-layer systems and mass transport through diffusion processes is required.

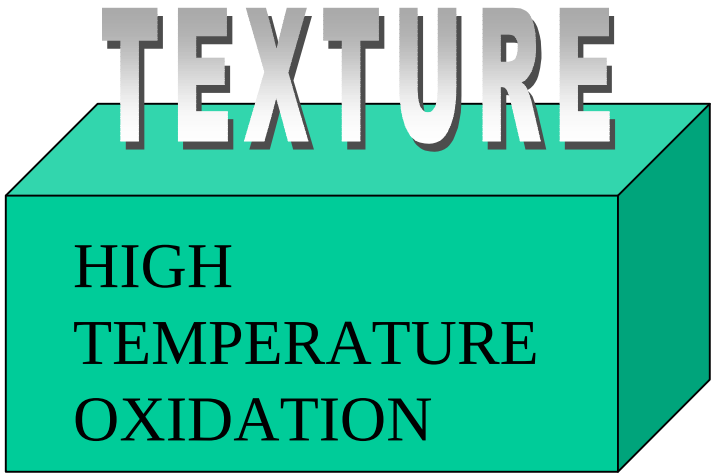
TEXTURE
HIGH
TEMPERATURE
OXIDATION

Kinetics of Oxidation on (100) and (111) Planes

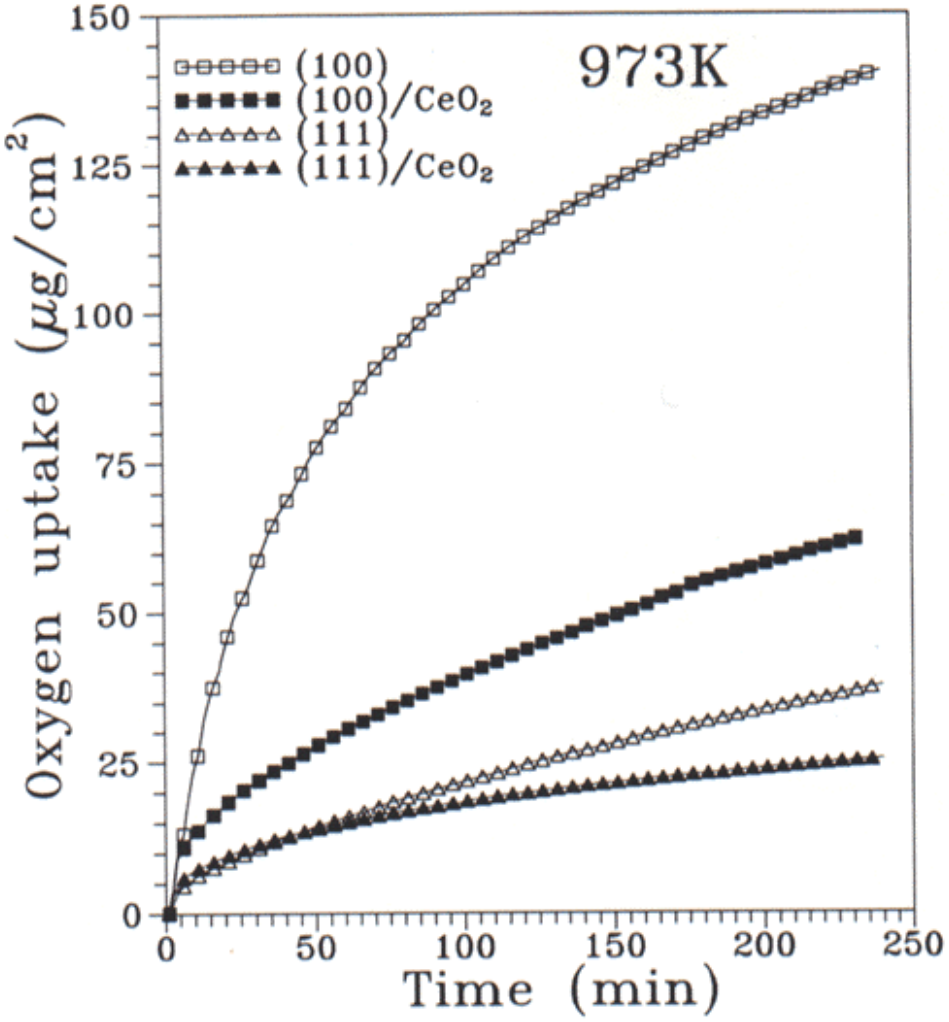

Oxidation of Polycrystalline Nickel

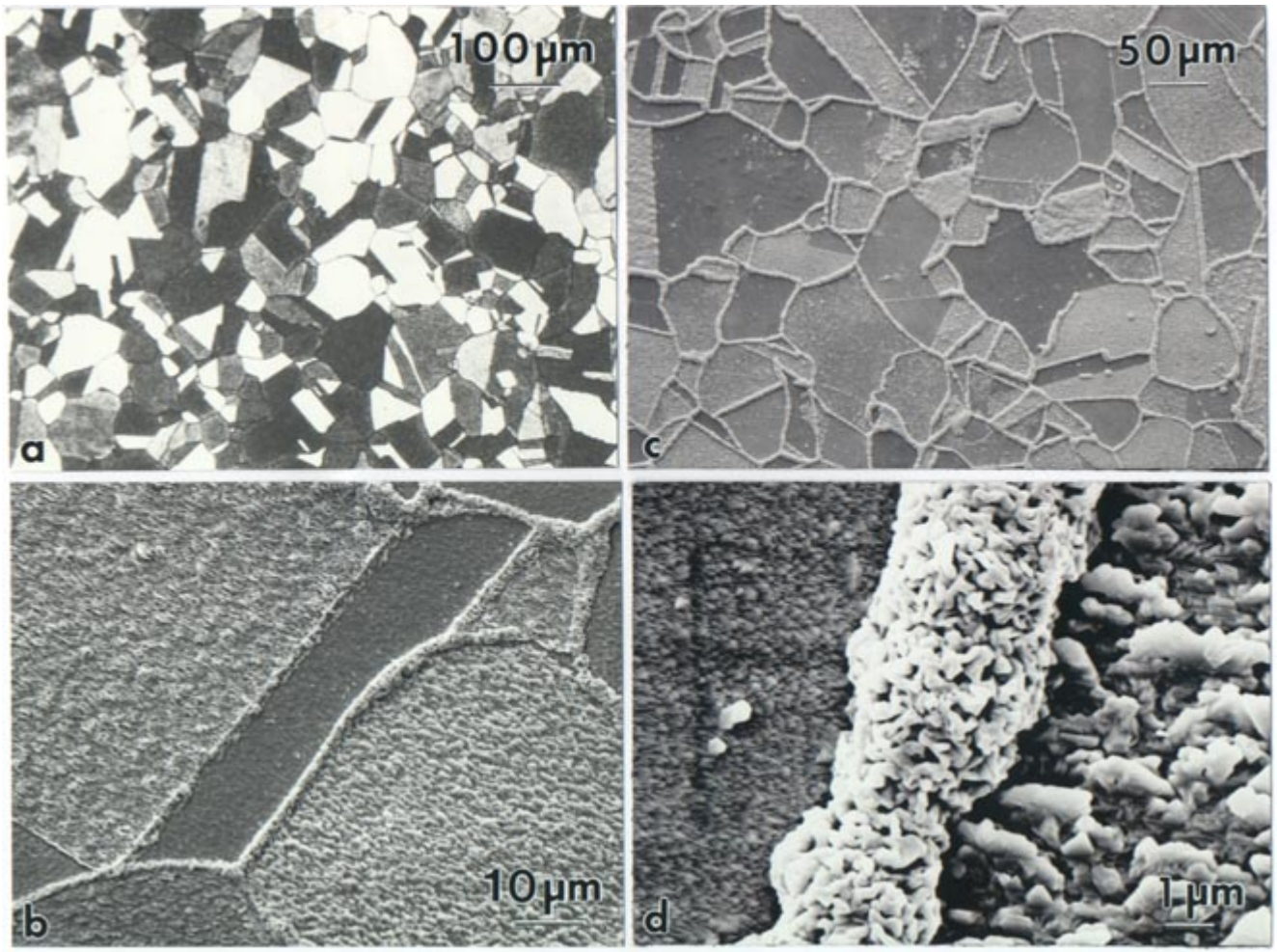

Oxidation at Grain Boundaries

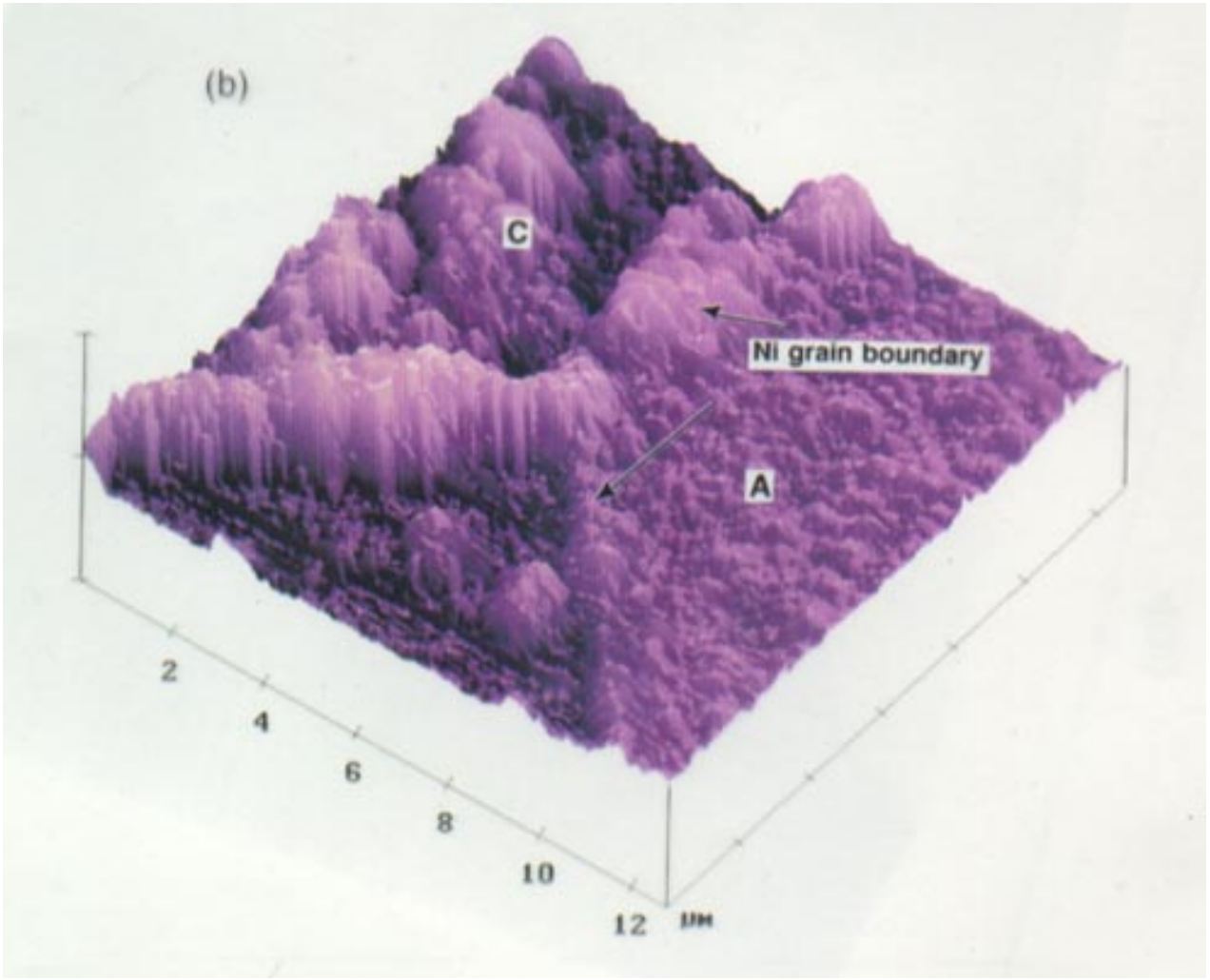

Cursor Marker Spectrum Zoom Center Line Offset Clear

Section Analysis

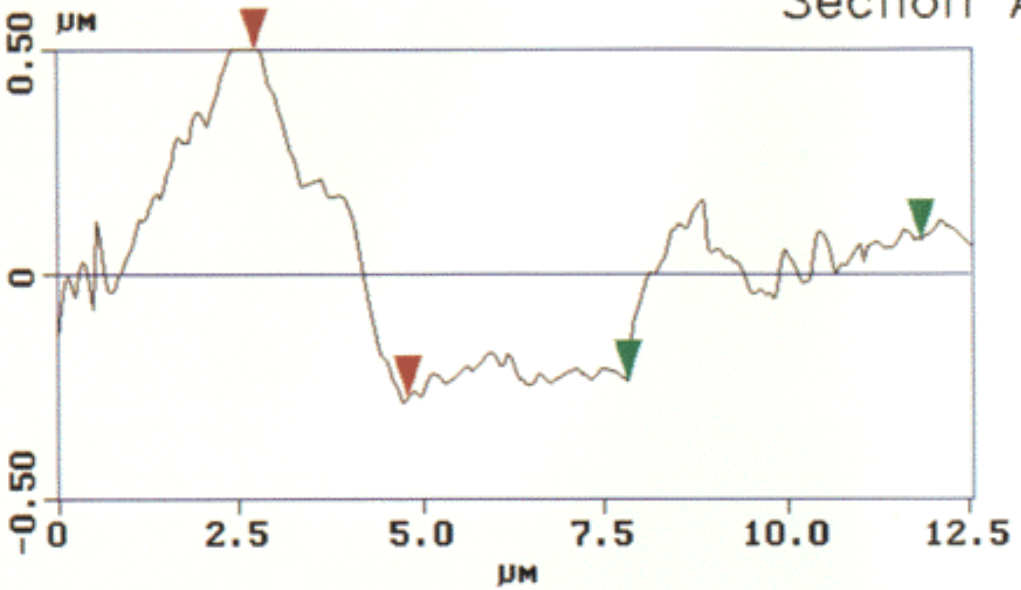

L	3.993 µm
RMS	63.215 nm
lc	264.65 nm
Ra(lc)	6.874 nm
Rmax	393.16 nm
Rz	147.18 nm
Rz Cnt	valid

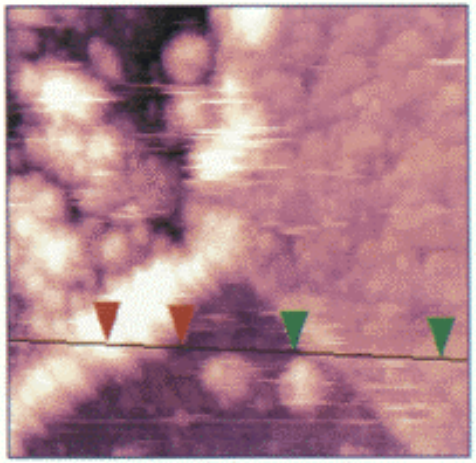

Spectrum

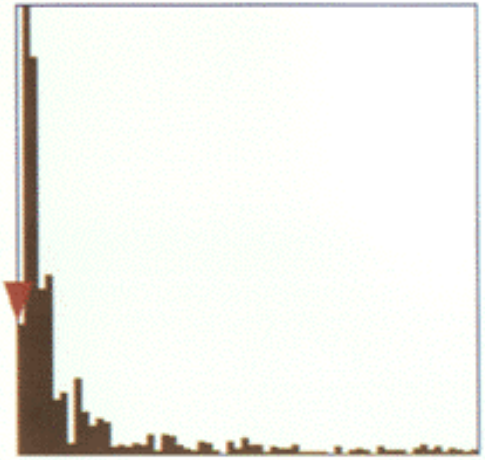

Horiz distance(L)	2.070 µm
Vert distance	806.51 nm
Angle	21.282 deg
Horiz distance	3.993 µm
Vert distance	316.31 nm
Angle	4.529 deg
Horiz distance	
Vert distance	
Angle	
Spectral period	264.65 nm
Spectral freq	283.95 Hz
Spectral amp	2.152 nm

Cursor: fixed Zoom: 8:1 Cen line: Off Offset: Off

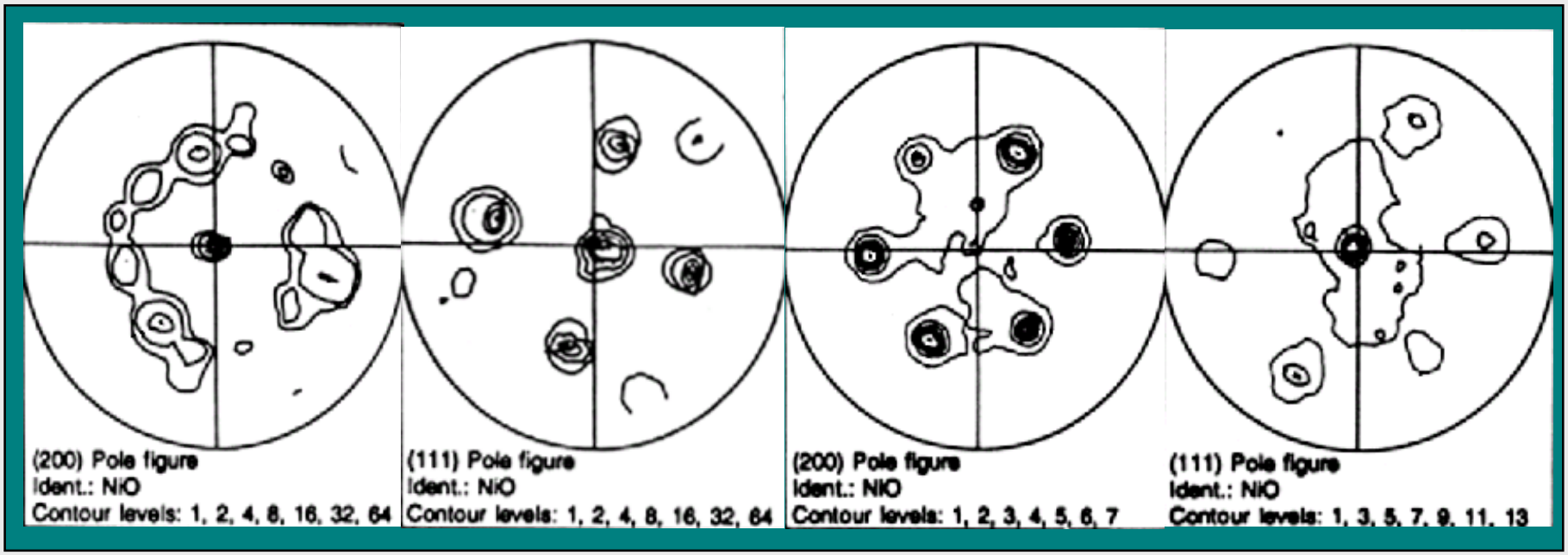
(200) Pole figure
Ident.: NiO
Contour levels: 1, 2, 4, 8, 16, 32, 64
(111) Pole figure
Ident.: NiO
Contour levels: 1, 2, 4, 8, 16, 32, 64
(200) Pole figure
Ident.: NiO
Contour levels: 1, 2, 3, 4, 5, 6, 7
(111) Pole figure
Ident.: NiO
Contour levels: 1, 3, 5, 7, 9, 11, 13

The proposed oxidation mechanism on Ni

- Nucleation occurs on the sample surface randomly, the orientations of the oxide nuclei are determined by the lattice matching between the oxide and the metal
- In the stage of oxide growth, the oxide grains with lower surface energy grow faster
- The re-nucleation occurs at the oxide grain boundary regions and the nucleation probability of an orientation is determined by its surface energy

$$p = \exp(-\beta \frac{E_{hkl}}{kT})$$

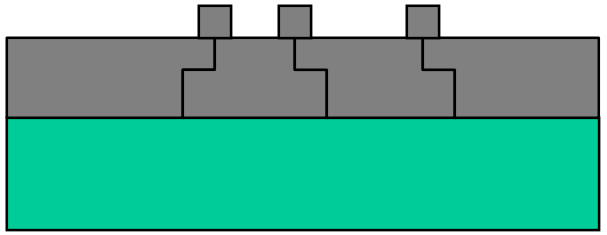

Application in Ni - NiO system

Early stage

$\{100\}_{Ni}$ $\{111\}_{Ni}$

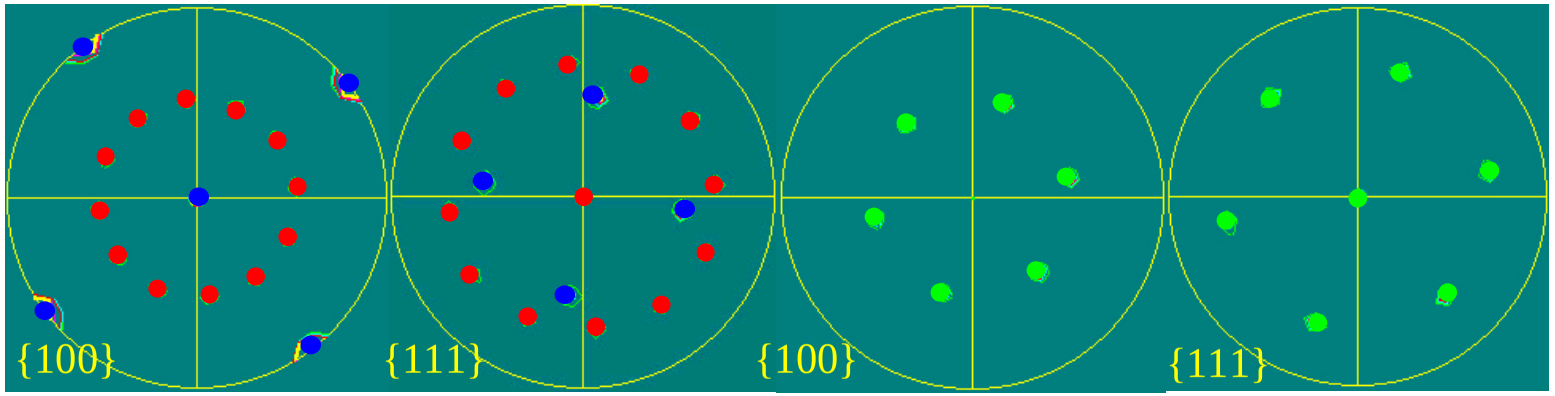

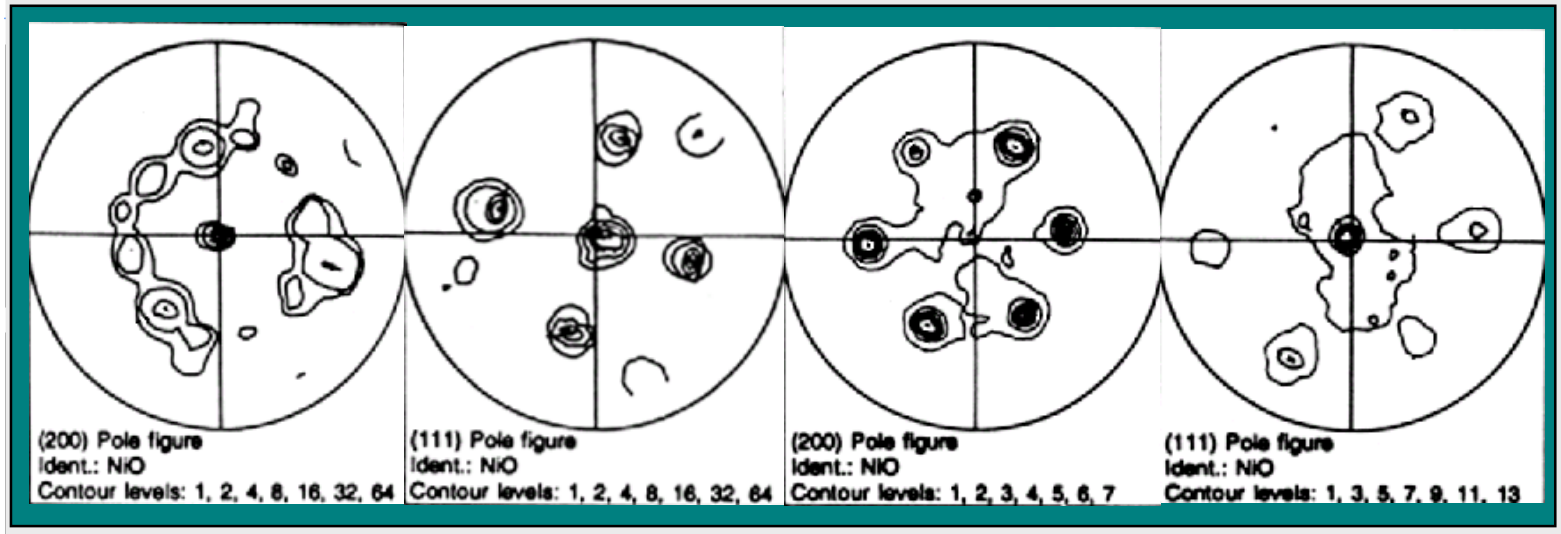

Computer Models

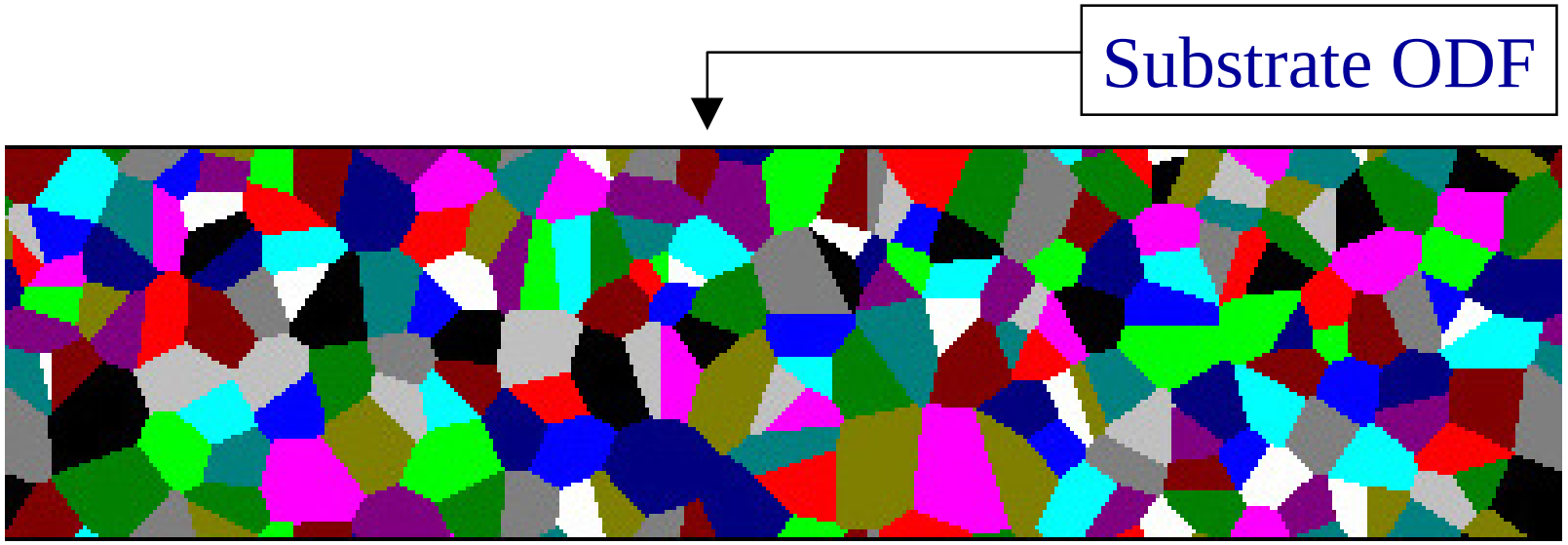

Substrate microstructure

- Substrate microstructure and ODF
- oxidation mechanism

Computer Models

Oxide microstructure

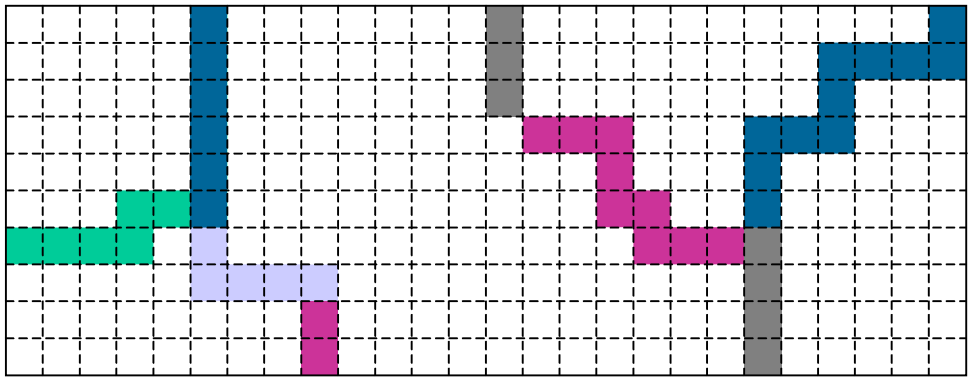

Random walk: $\Gamma = nD(x, y)/\Delta x^2$

Interface

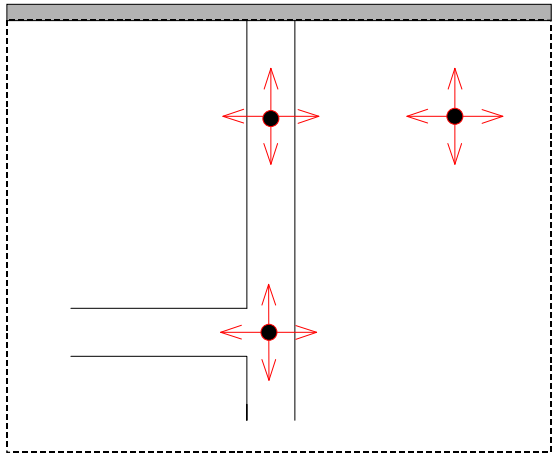

- Oxide microstructure and texture
  (Grain boundary character distribution)
- Diffusion coefficient as a function of grain boundary character

Application in Ni - NiO system

Effects of oxide texture and microstructure on the oxidation kinetics

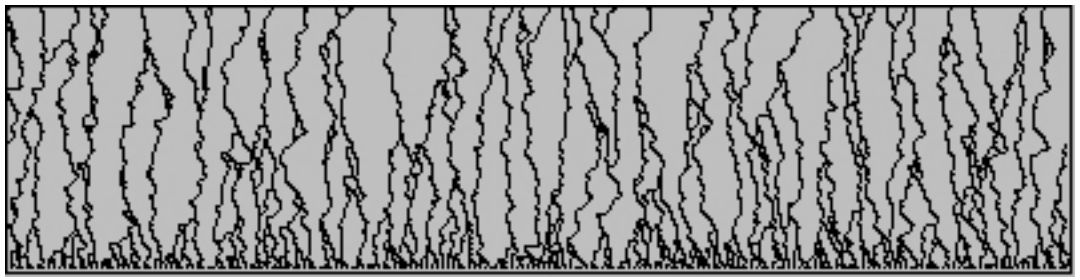

53% Σ3

$D_{\Sigma 3}=D_{bulk}=5.5\times10^{-15}$ cm^2/s

$D_{gb}=7.5\times10^{-10}$ cm^2/s

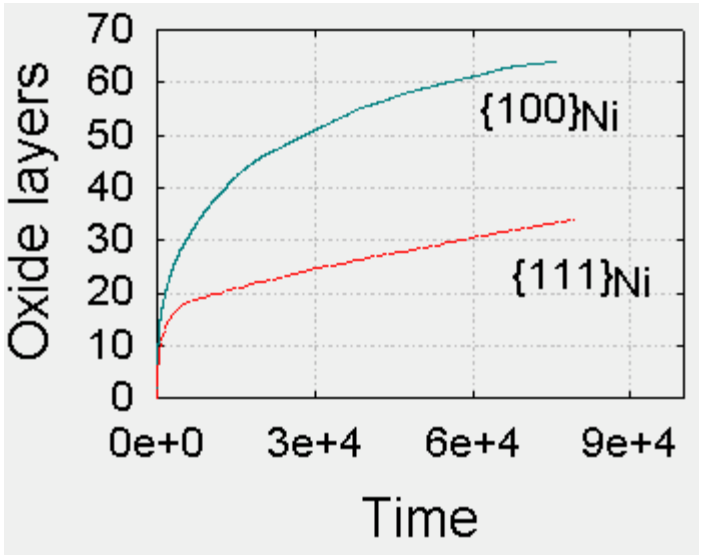

$K_{100}:K_{111}=10:1$

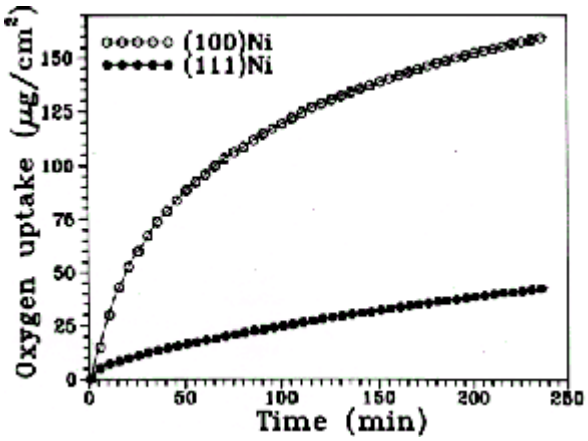

$K_{100}:K_{111}=14:1$

Message

- Control of surface texture can be used to slow down high temperature oxidation in Nickel based and other alloys alloys
- Further research is needed to understand the process of oxide texturing and diffusion of oxygen and metal through the oxide.


TEXTURE
HYDROGEN INGRESS THROUGH ZIRCONIA FILMS

OPERATIONAL ENVIRONMENT OF THE Zr-2.5%Nb PRESSURE TUBE

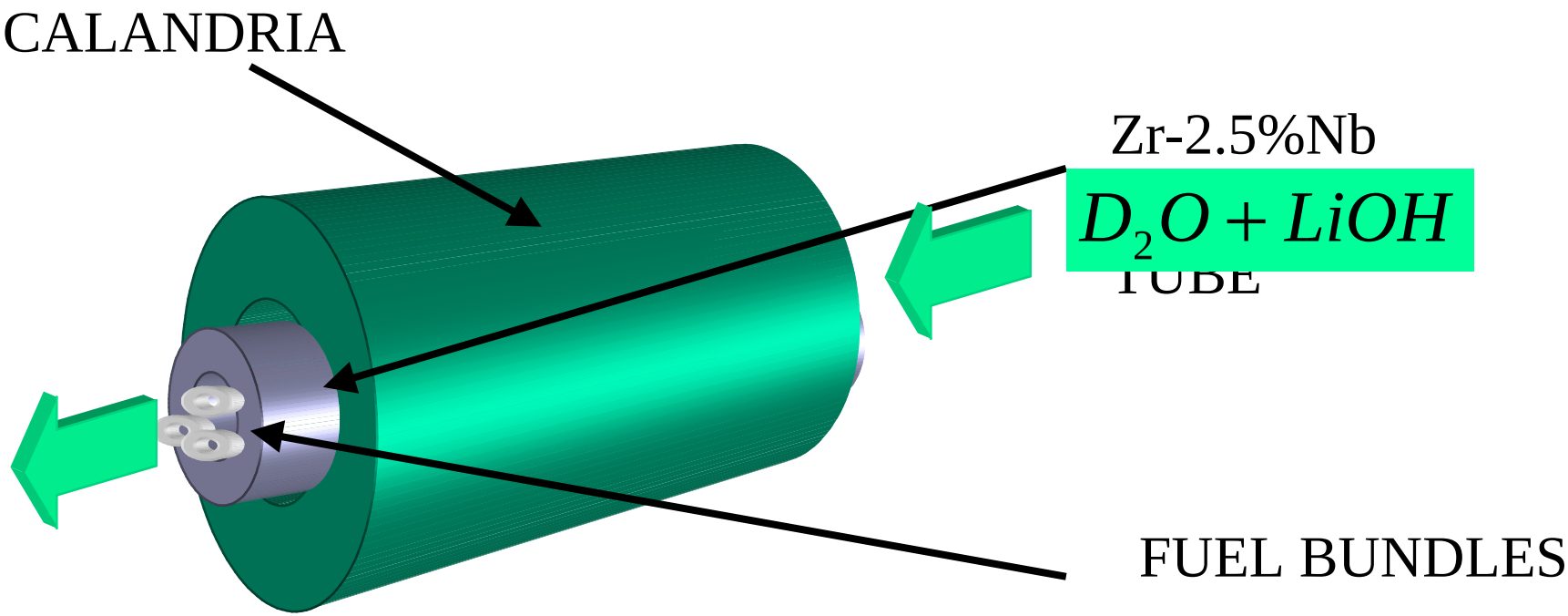

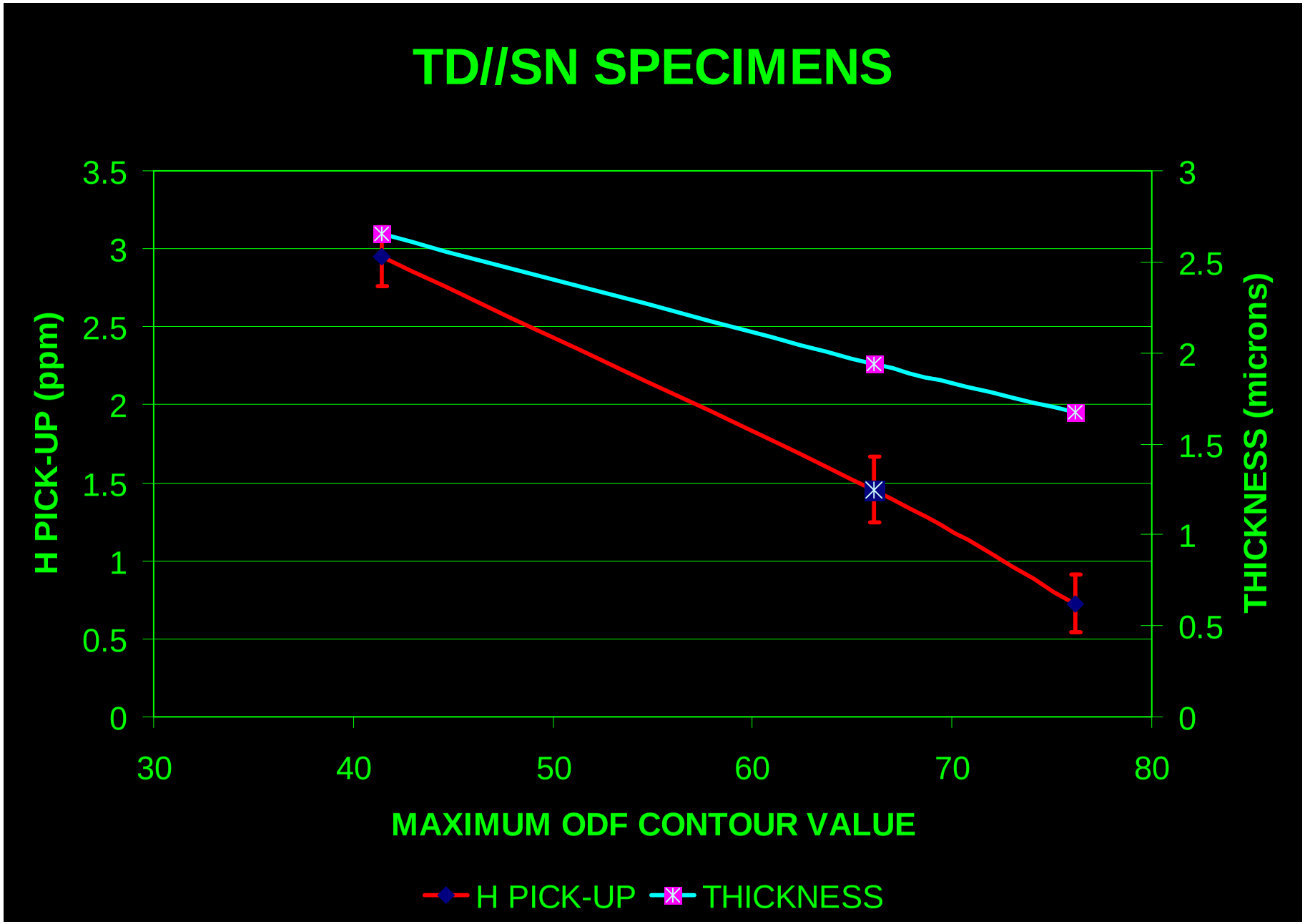
TD//SN SPECIMENS
H PICK-UP (ppm)
THICKNESS (microns)
3.5
3
2.5
2
1.5
1
0.5
0
3
2.5
2
1.5
1
0.5
0
30
40
50
60
70
80
MAXIMUM ODF CONTOUR VALUE
H PICK-UP
THICKNESS

The proposed mechanism of Zr-2.5%Nb oxidation

- Nucleation occurs on the sample surface randomly, the orientations of the oxide nuclei are determined by the lattice matching between the oxide and the metal
- In the stage of oxide growth, minimization of the stress, parallel to the sample surface, plays a main role.
- The re-nucleation occurs at the α-Zr grain boundary and β-Zr regions and the oxide orientation is determined by lattice matching

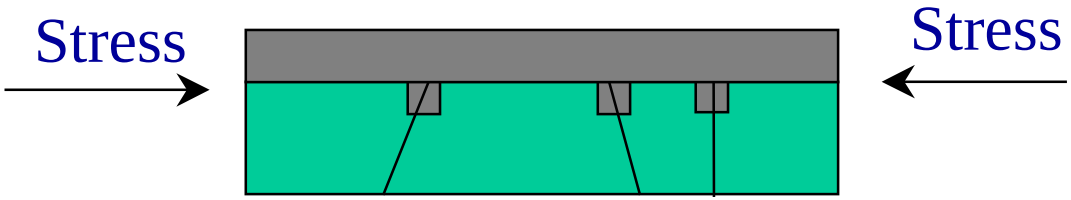

Application in Zr - ZrO_2 system

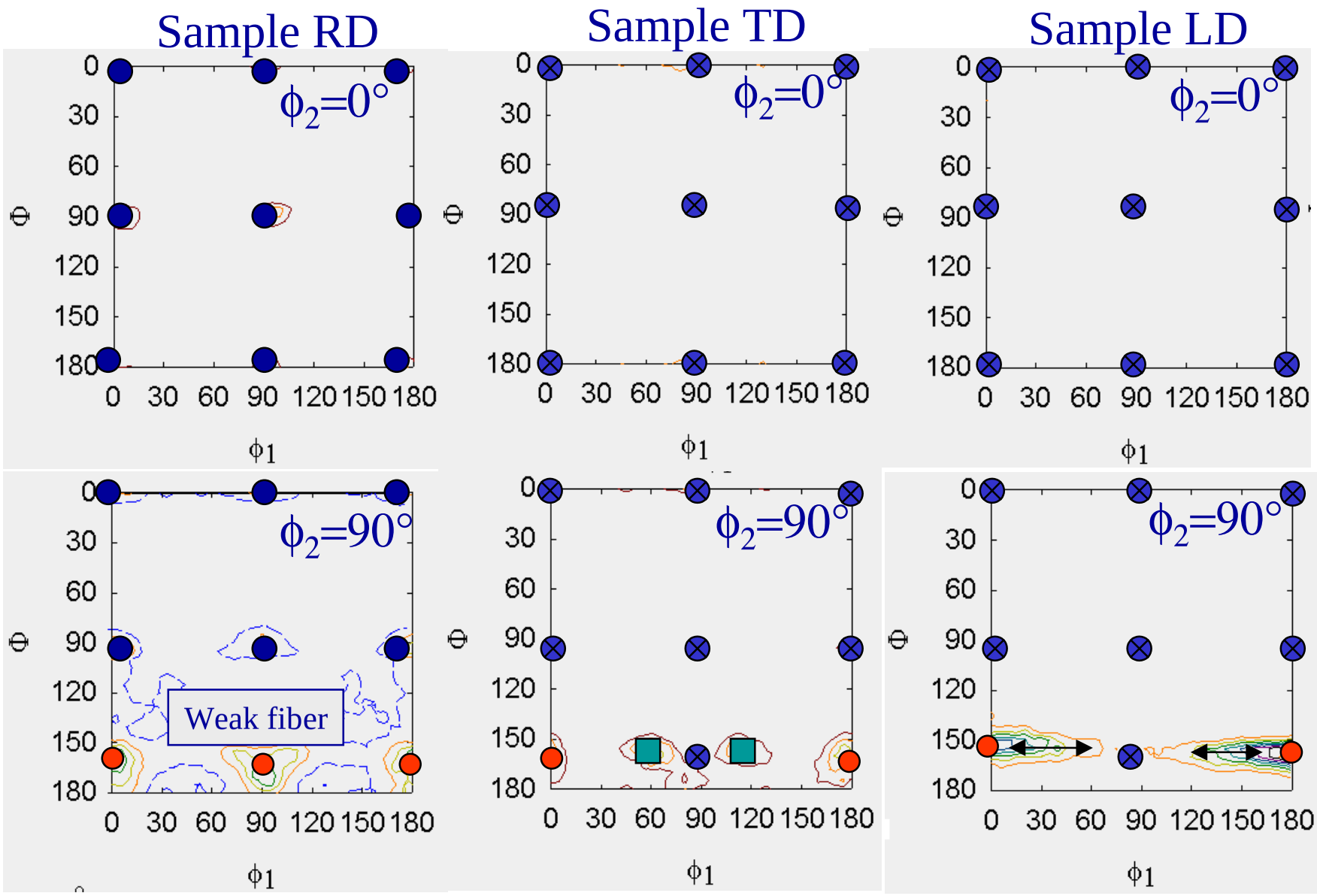

Application in Zr - ZrO_2 system

Oxide microstructure

- In the bulk of α-Zr grain
- At the α-Zr grain boundary
- In β-Zr region

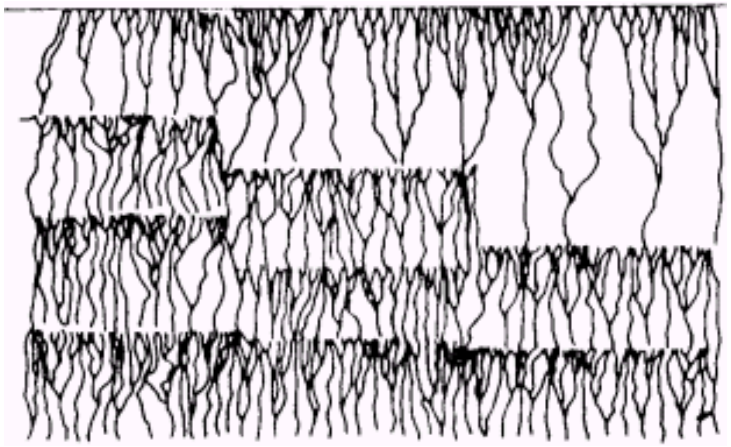

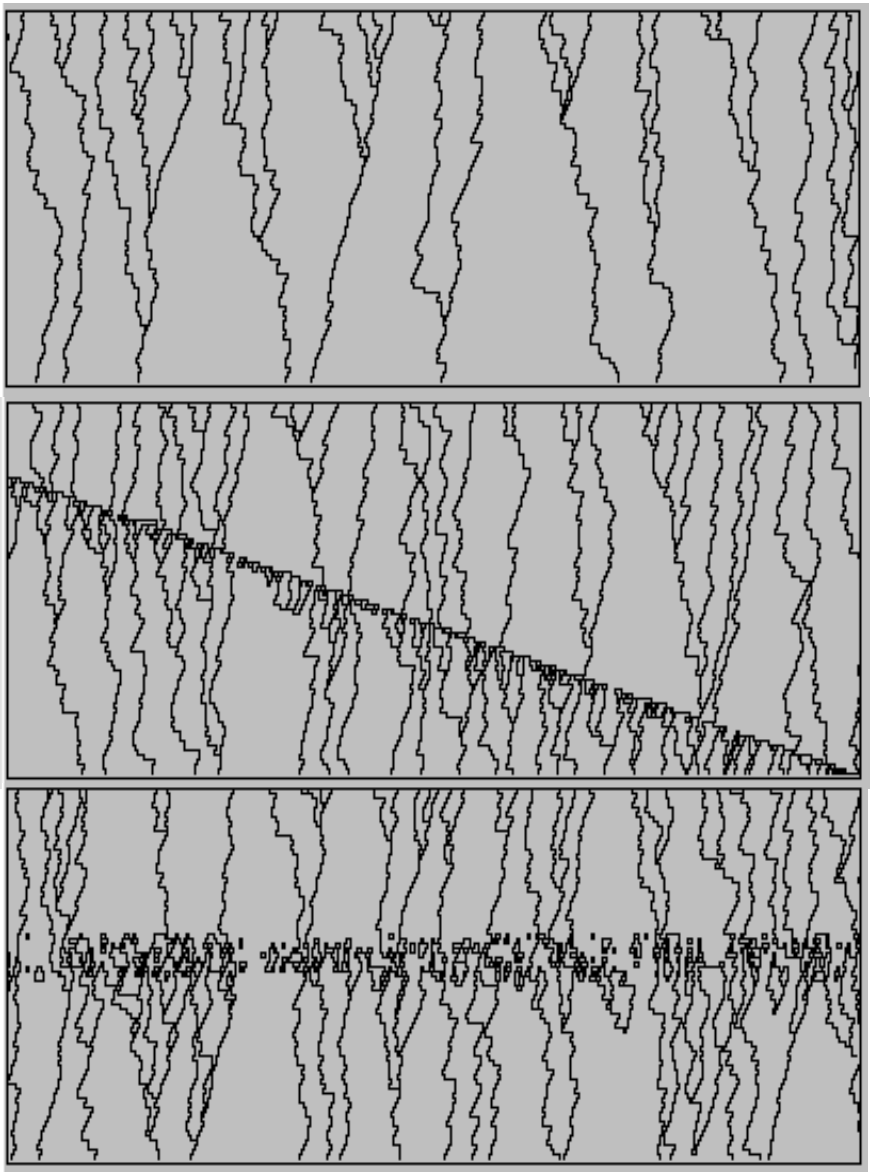

Application in Zr - ZrO_2 system

Diffusion mechansim in ZrO_2

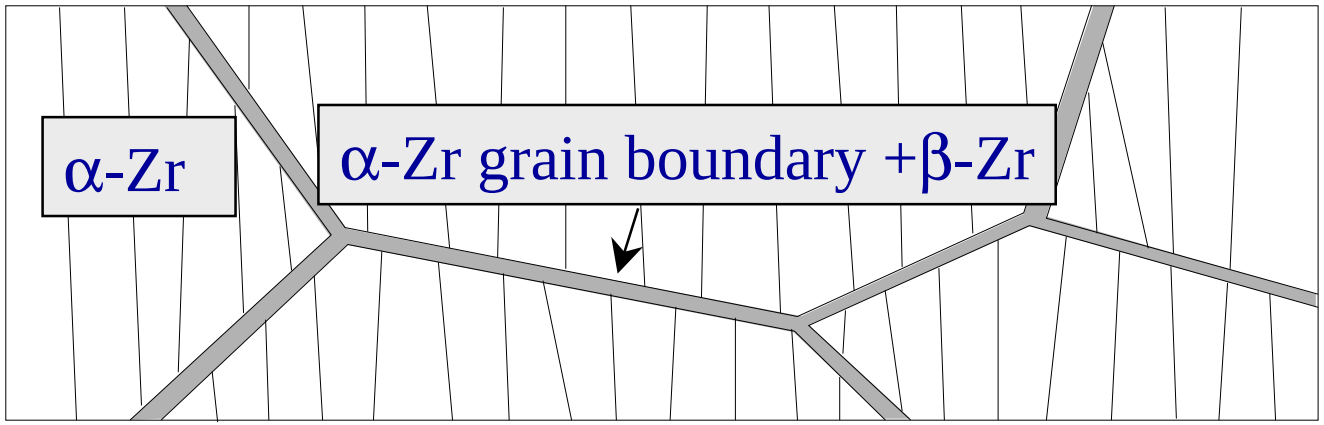

The first diffusion path The second diffusion path

Application in Zr - ZrO_2 system

Simulation of oxidation kinetics

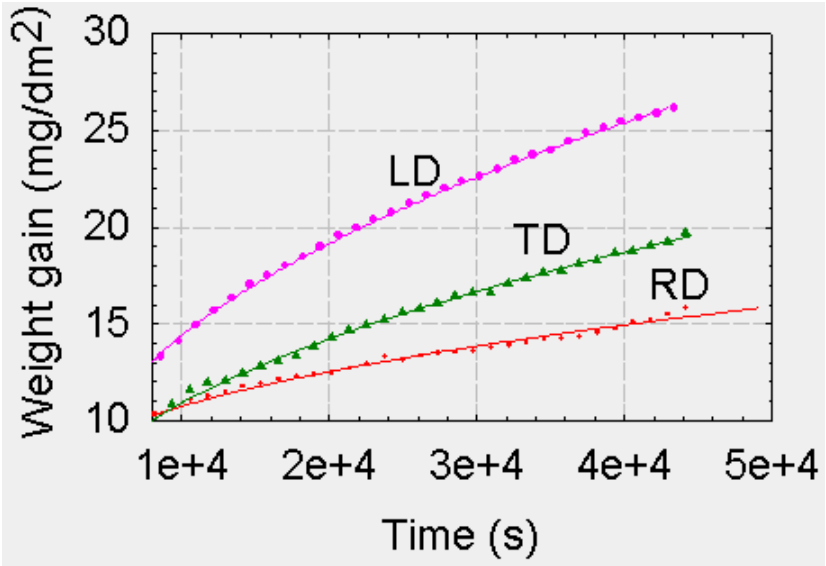

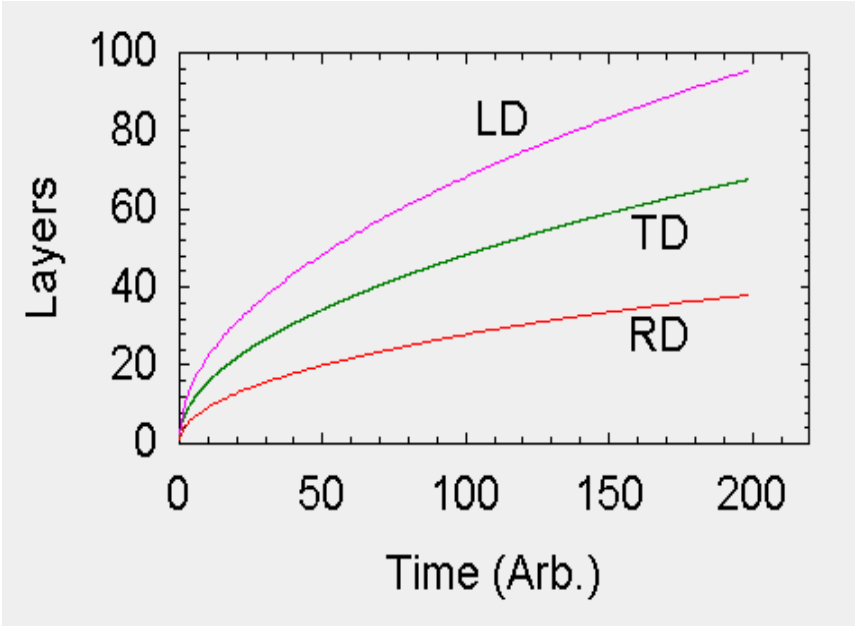

$K_{RD}:K_{TD}:K_{LD}=1:3:6$

$K_{RD}:K_{TD}:K_{LD}=1:2.8:5.6$

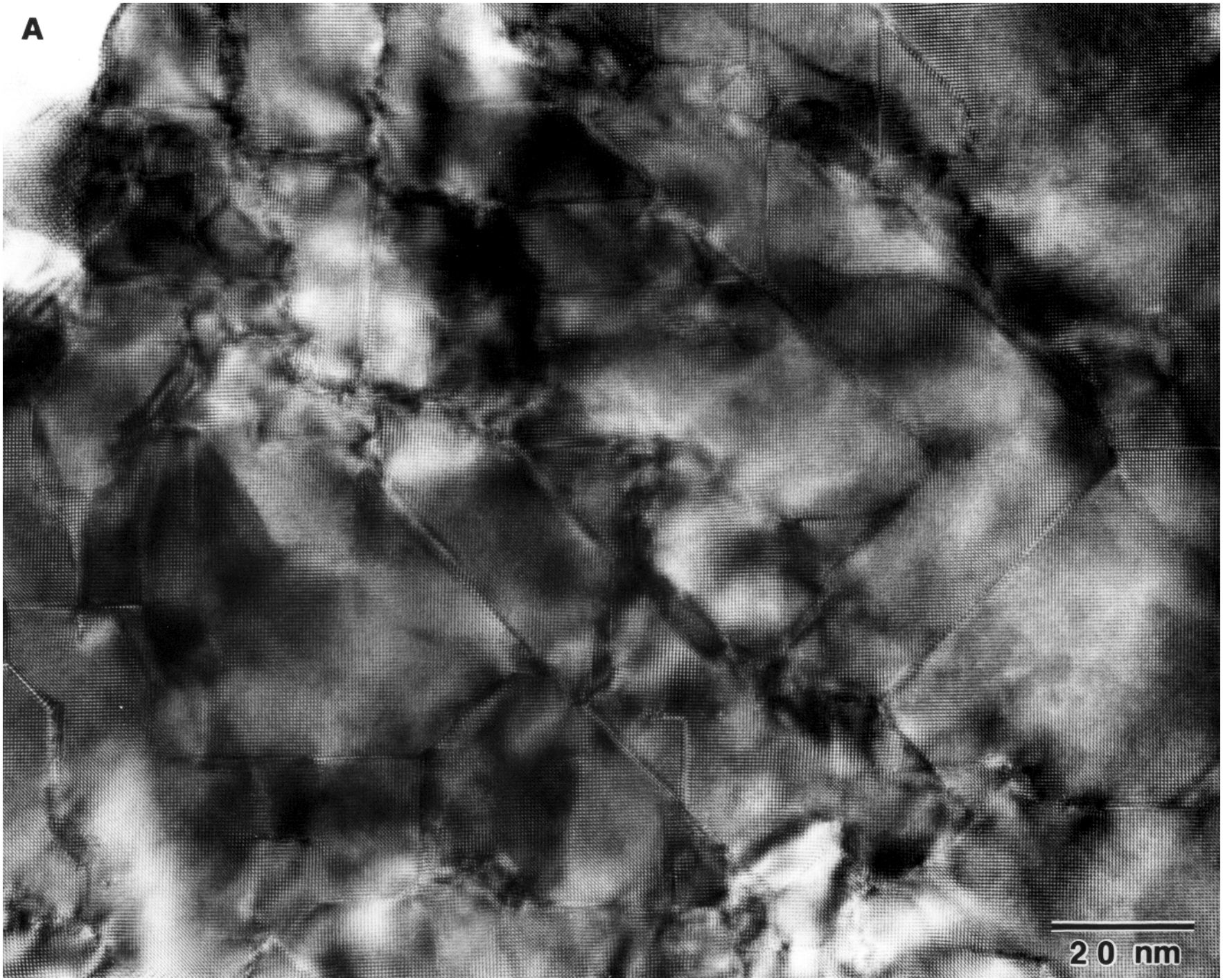
A
20 nm

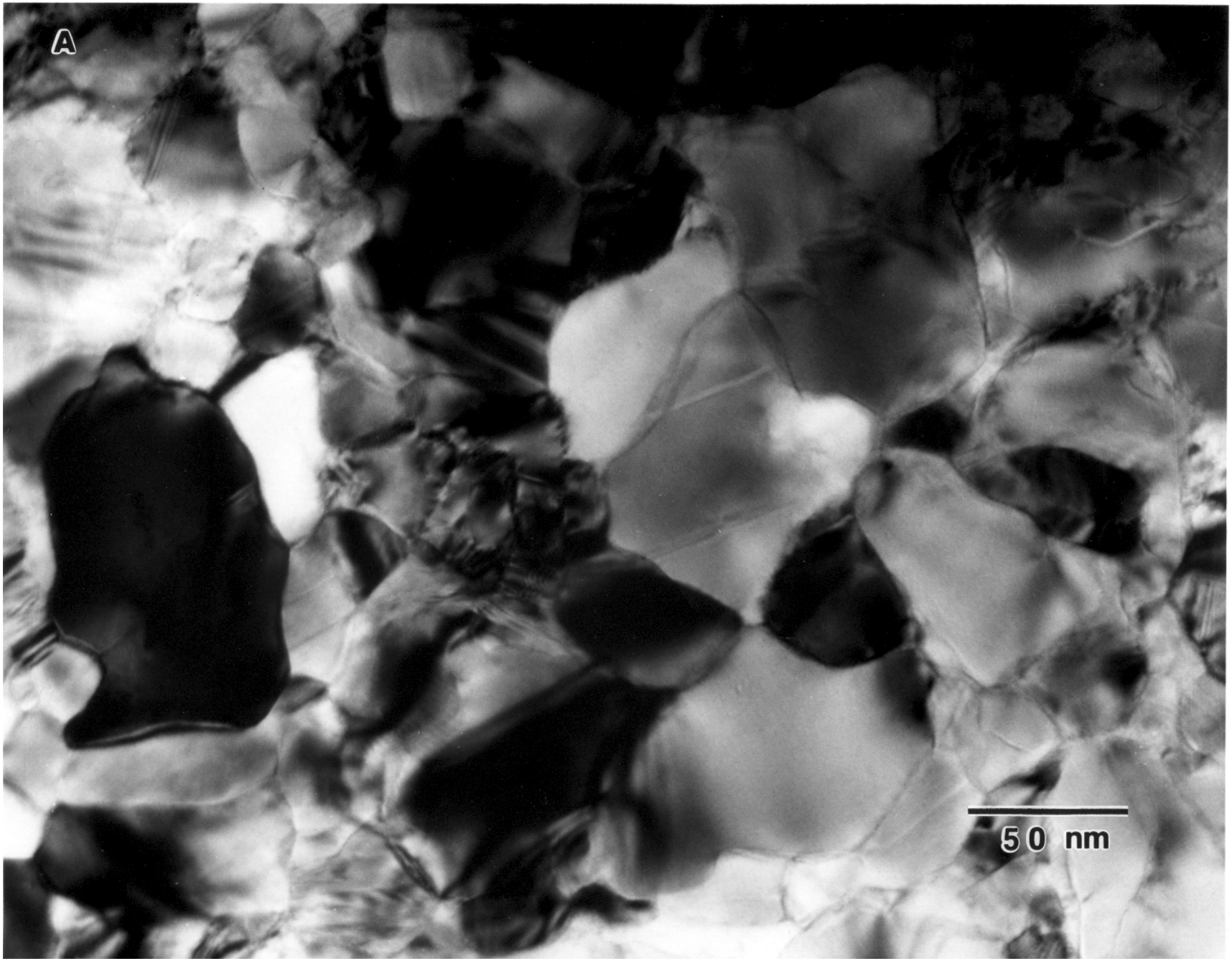
A
50 nm

Typical Interfacial Configurations in Zirconia Film

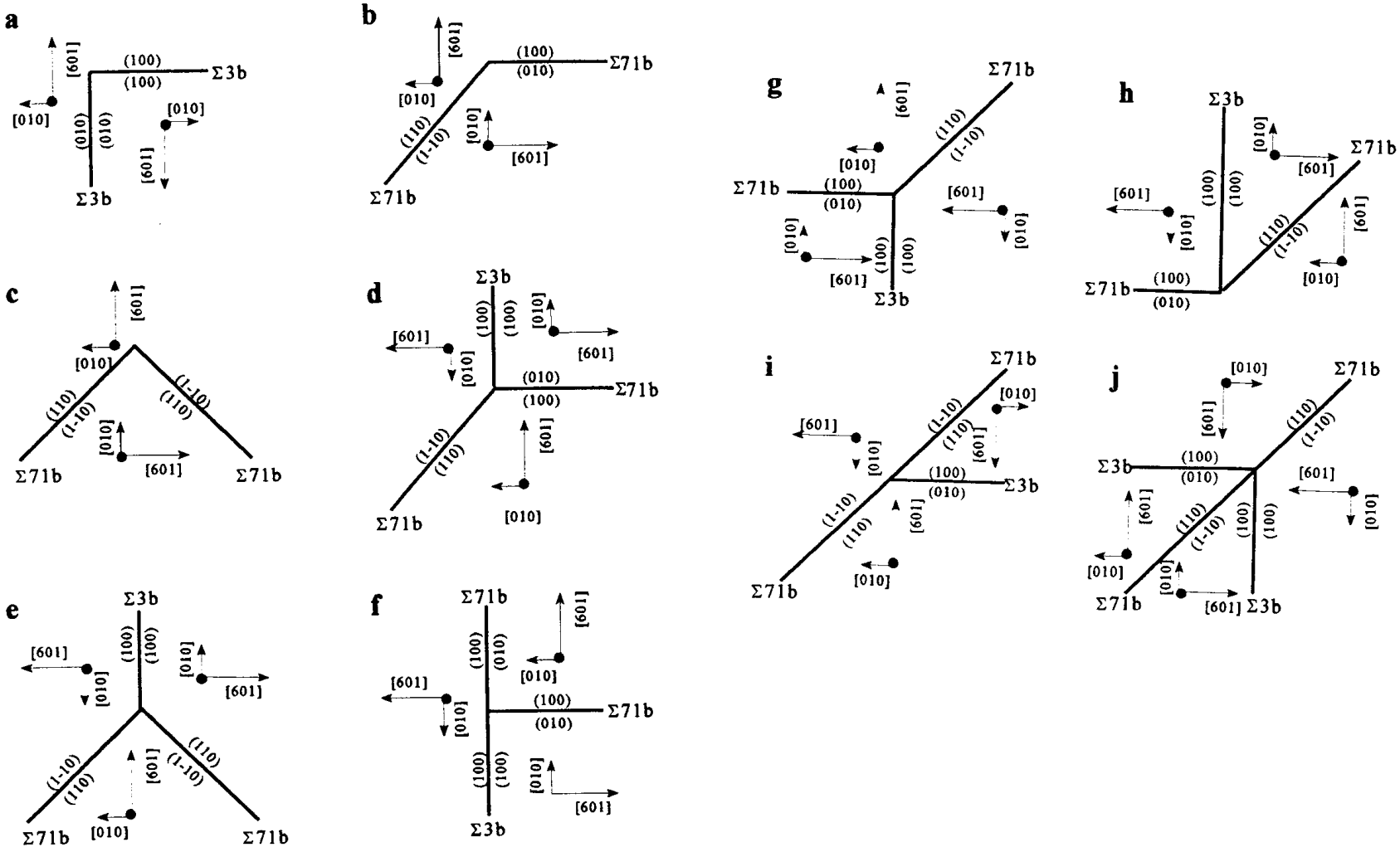

Σ71b
Σ3b
Σ71b
(100)
(010)
(110)
(1-10)
(010)
(100)
(100)
(010)
(110)
(1-10)

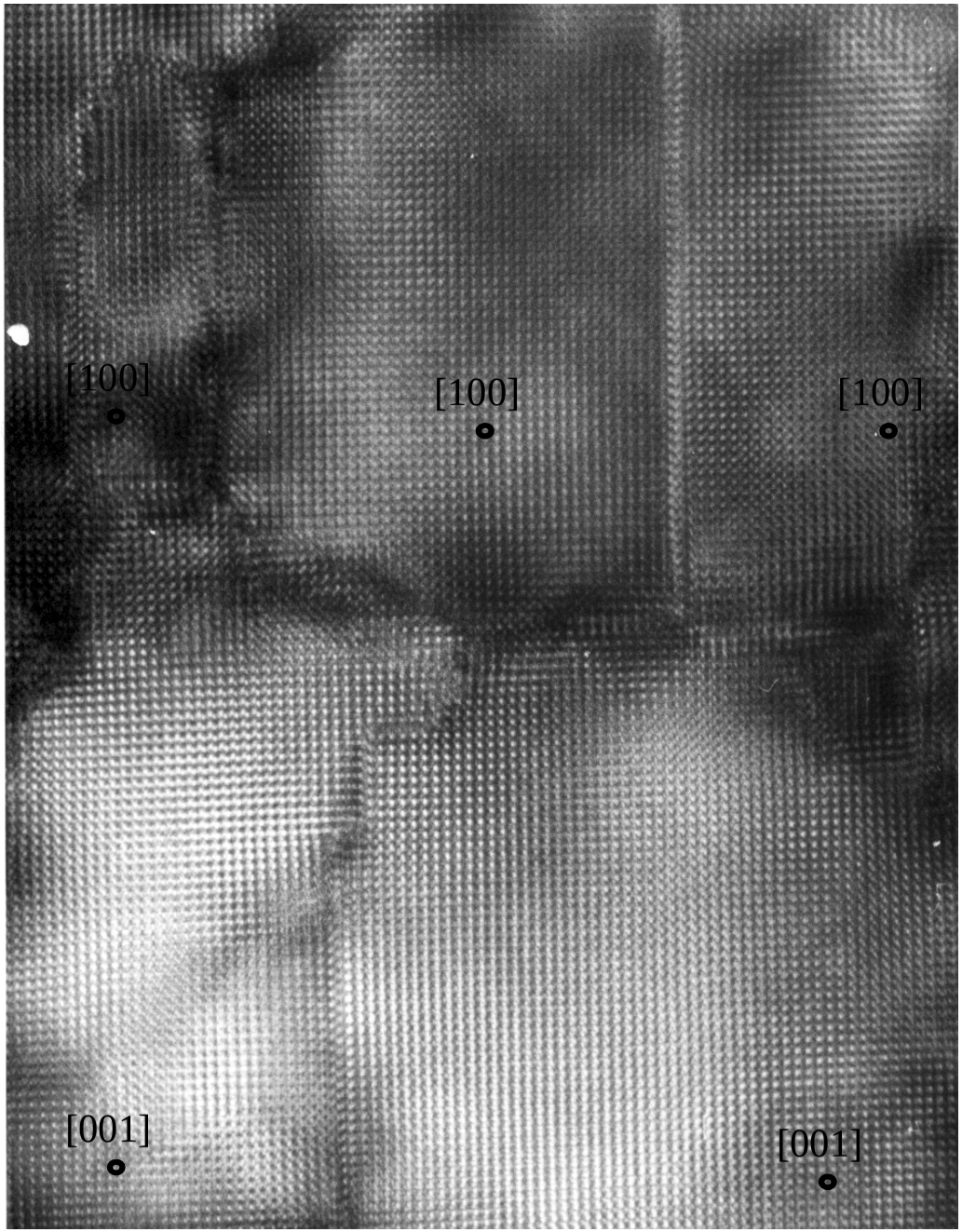
[100]
[100]
[100]
[001]
[001]

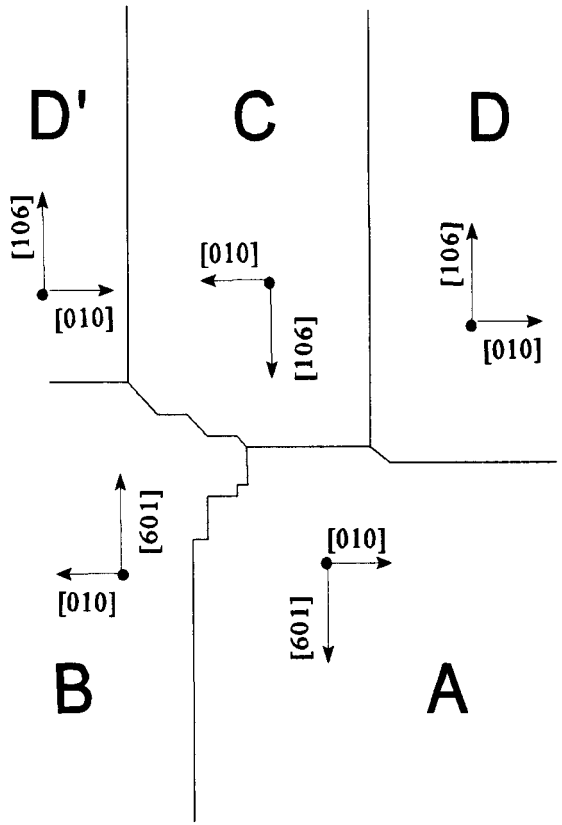

Misorientations:

A/B	Σ3b:	180°[001]=180°[601]
C/D and C/D′	Σ3a:	180°[100]=180°[106]
A/C and B/D′	Σ1′:	180°[101]=180°[$10\bar{1}$]
A/D and B/C	Σ3c:	80.4°[010]=99.6°[010] (rotation by the β angle about [010])

Message

- High resistance of Zirconium to corrosion and hydrogen permeation is due to a specific “growth mode” texture
- One has to learn how to grow strong oxide texture and how to control the orientation of zirconium alloy substrate.

Application in Ni - NiO system

Oxide microstructure

On $\{100\}_{Ni}$

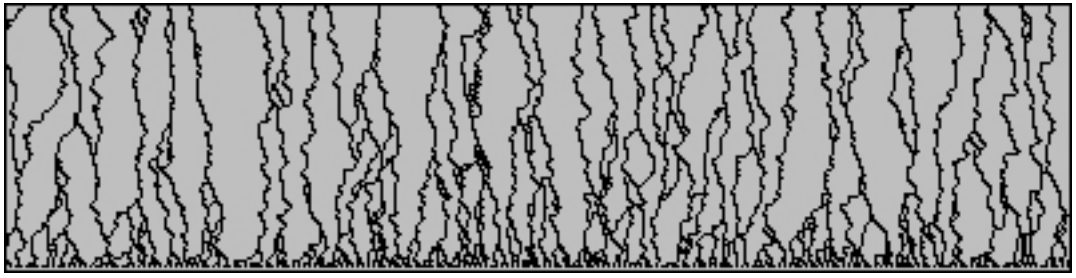

On $\{111\}_{Ni}$

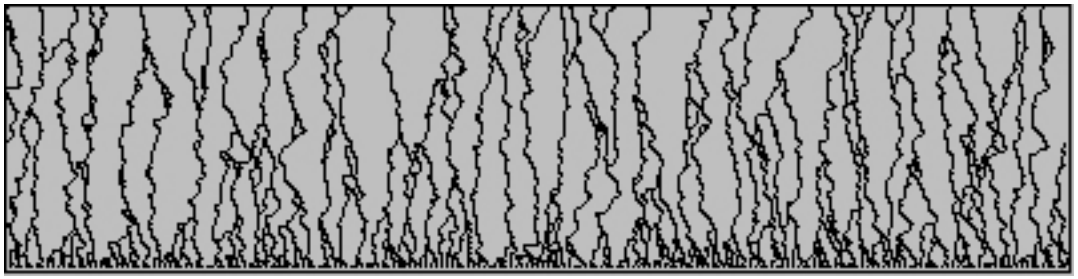

Experimental microstructure

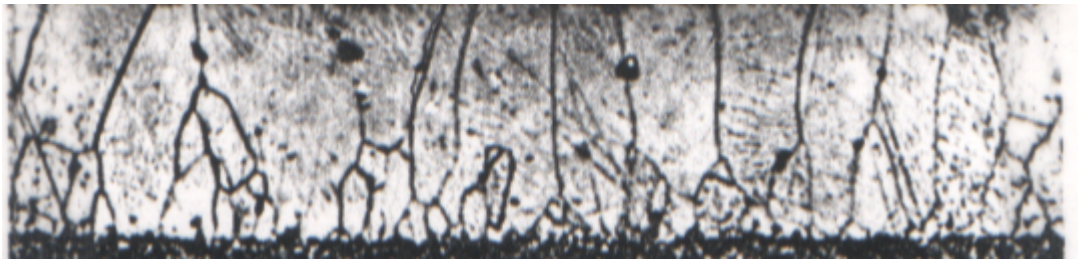

STEAM FORMED OXIDES

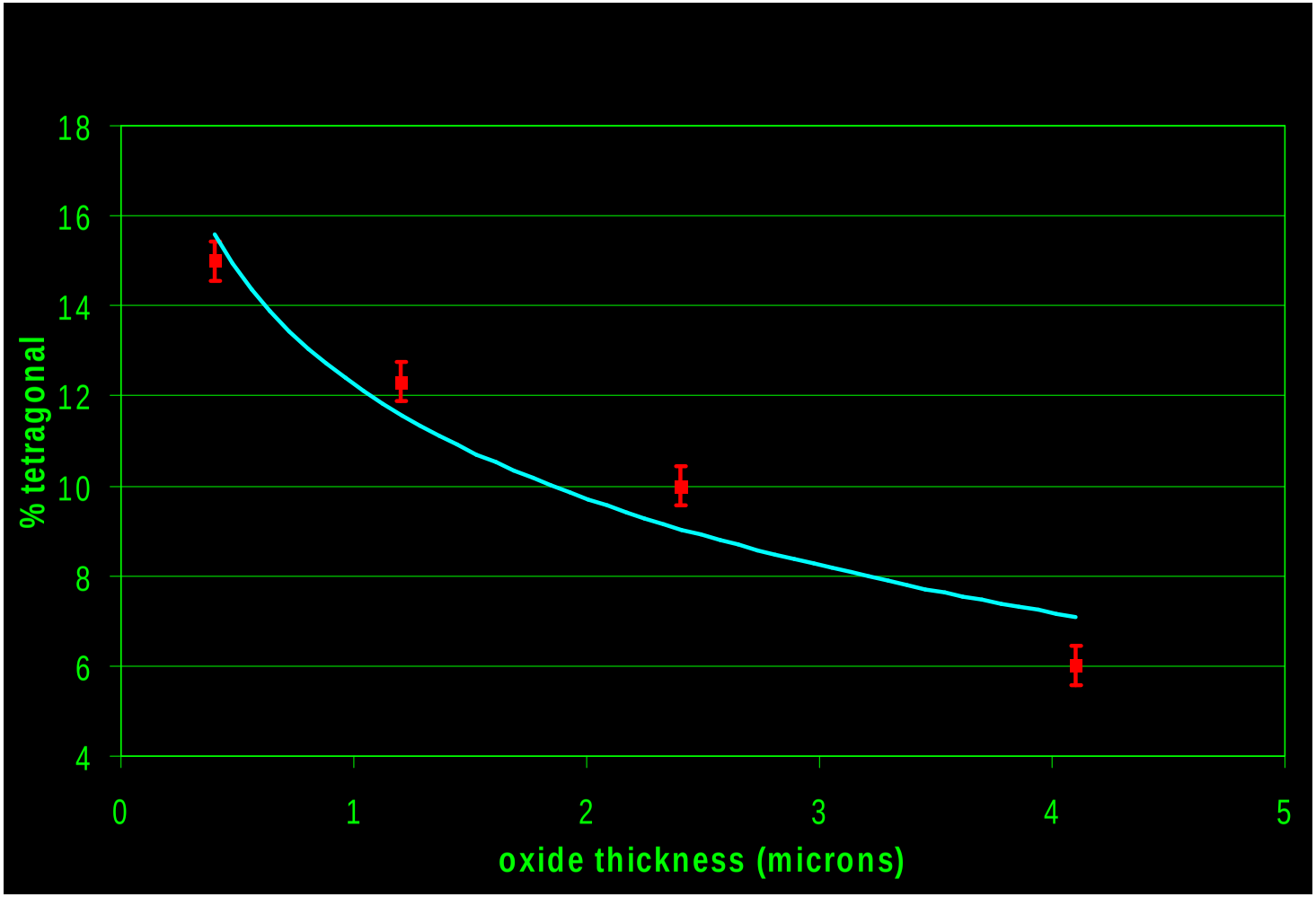

tmquen48.021

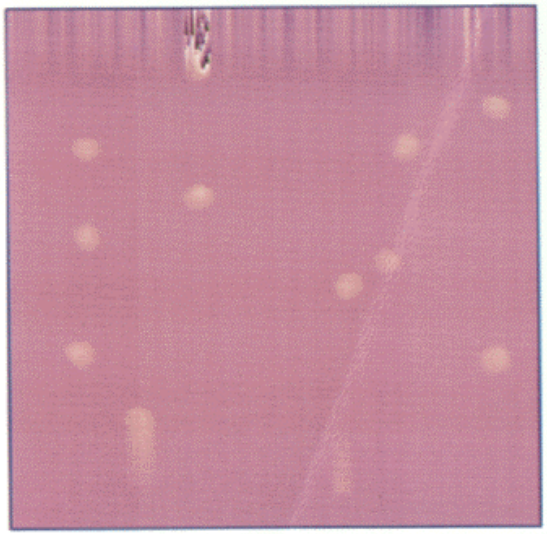

tmquen44.001

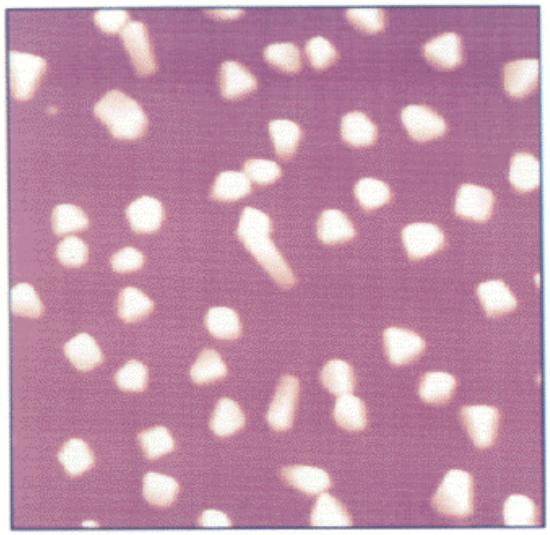

tmquen49.001

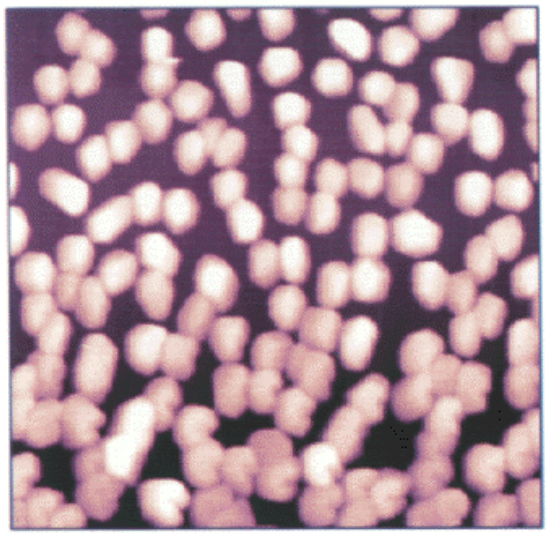

tmquen46.001

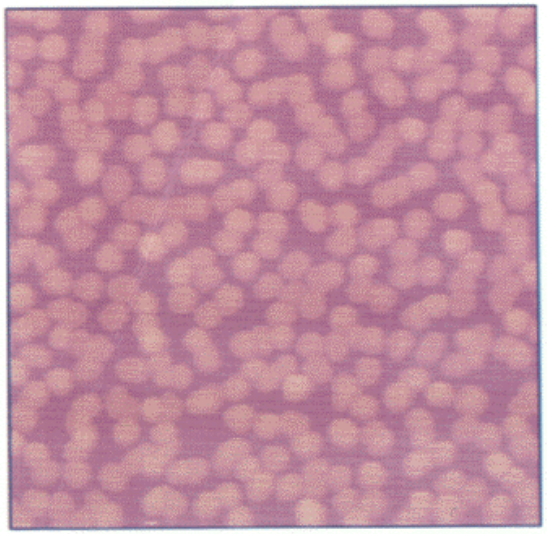

tmquen51.002

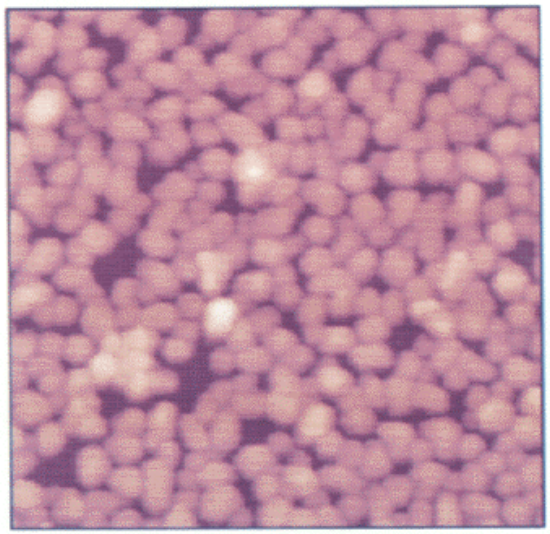

Application in Ni - NiO system

In the stage of growth and re-nucleation

(*hkl*)	Surface energies (J/m^2)
(100)	12.6
(111)	17.7
(110)	17.8
(210)	24.8
(211)	20.0
(221)	30.7
(311)	27.3

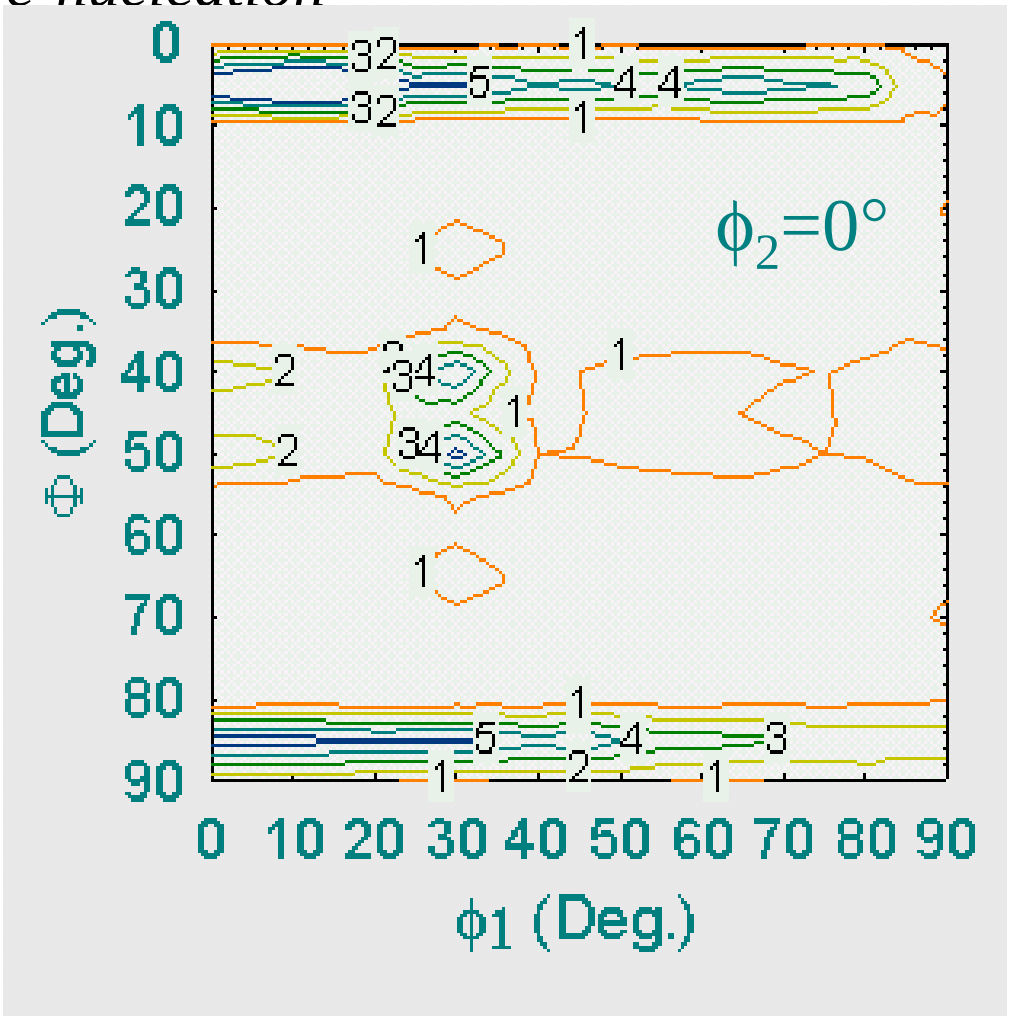

Calculated oxide ODF from experimental pole figures

Application in Ni - NiO system

Effects of oxide texture and microstructure on the oxidation kinetics

Grain boundary character distribution

- random grain boundary
- Σ3 (twin) boundary (60° along <111>)

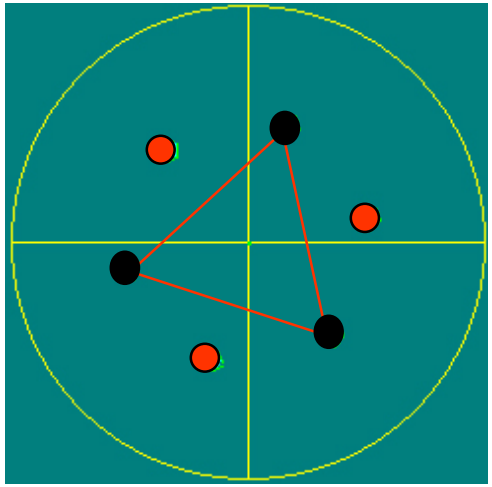

{100} pole figure of the oxide grown on $\{111\}_{Ni}$

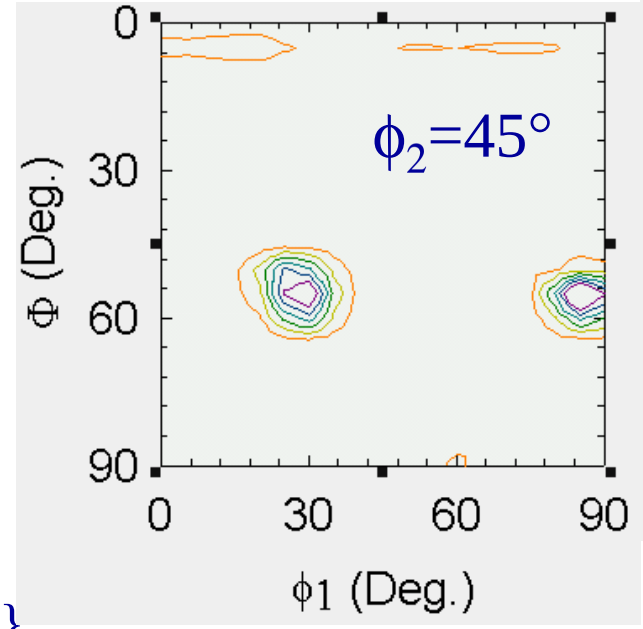

Structure of Σ3 grain boundary

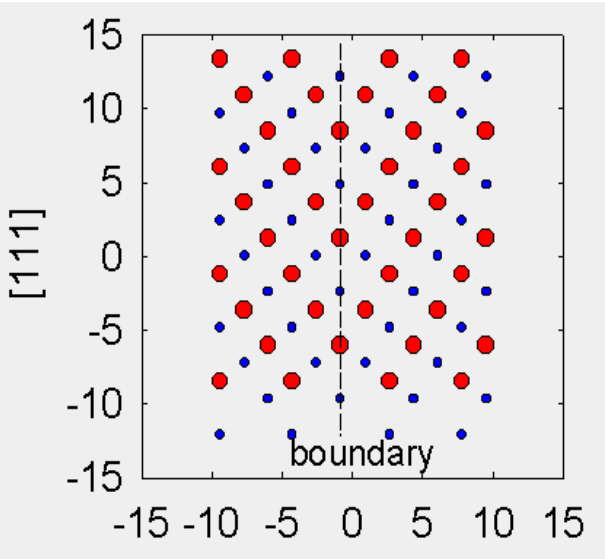

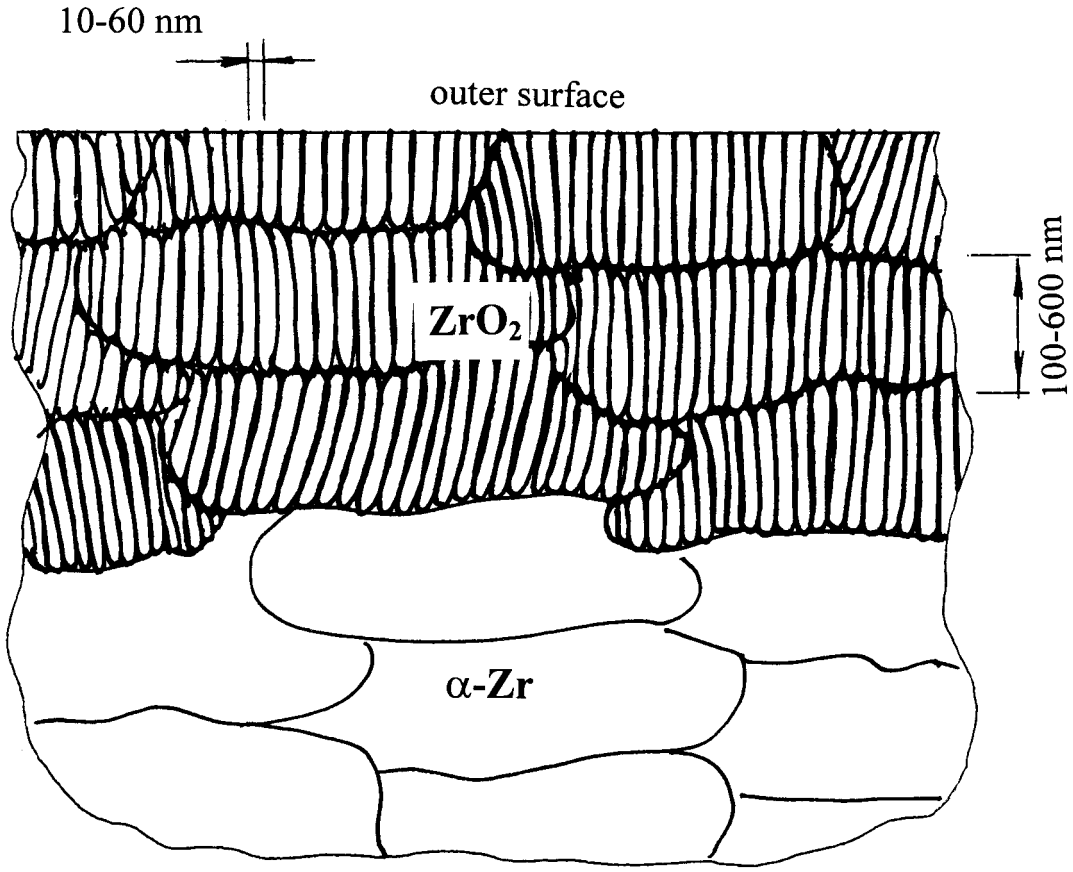
10-60 nm
outer surface
ZrO_2
100-600 nm
α-Zr

Application in Zr - ZrO_2 system

On RD sample

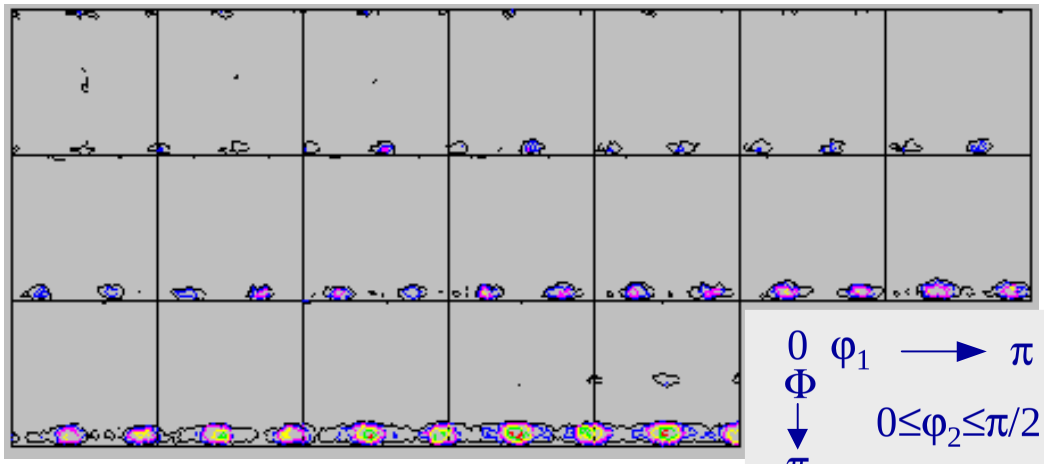

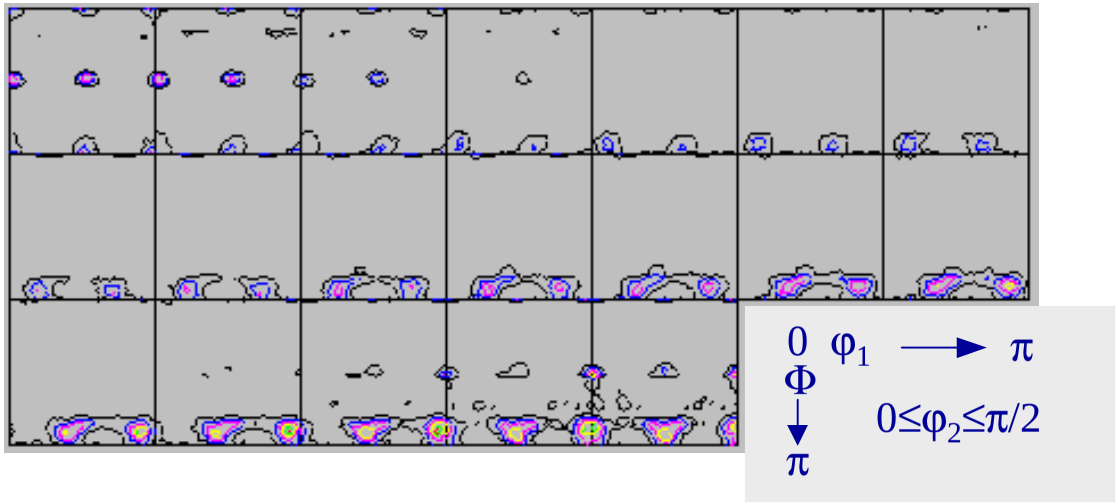

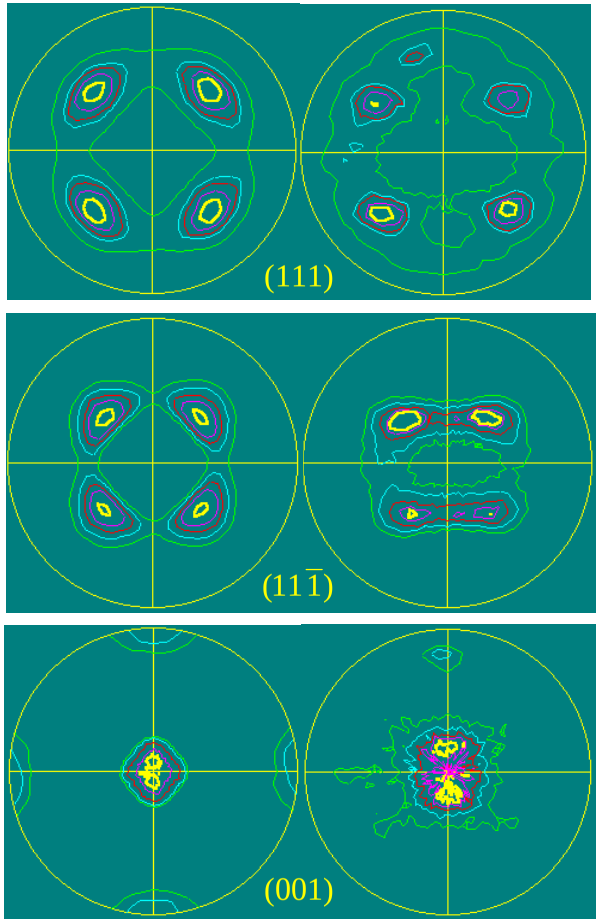

Application in Zr - ZrO_2 system

On TD sample

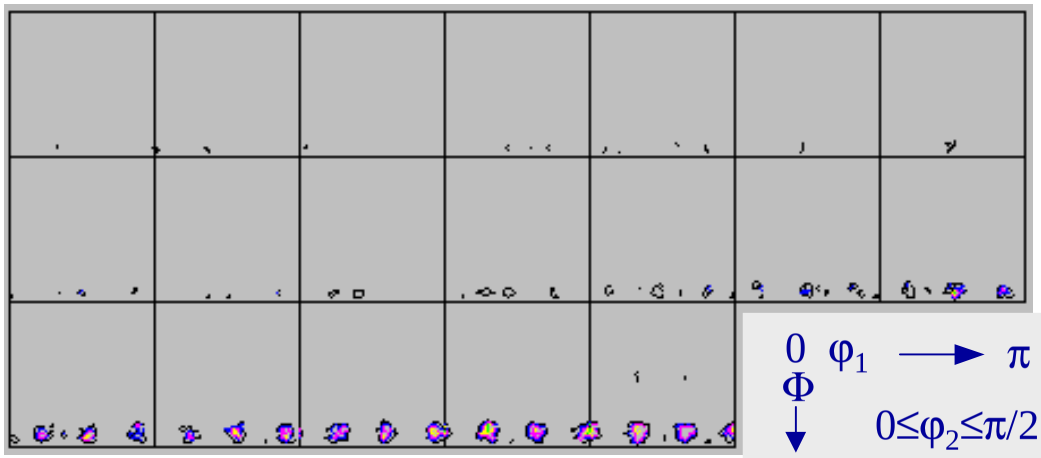

$0 \le \varphi_1 \le \pi$

Φ: $0 \rightarrow \pi$

$0 \le \varphi_2 \le \pi/2$

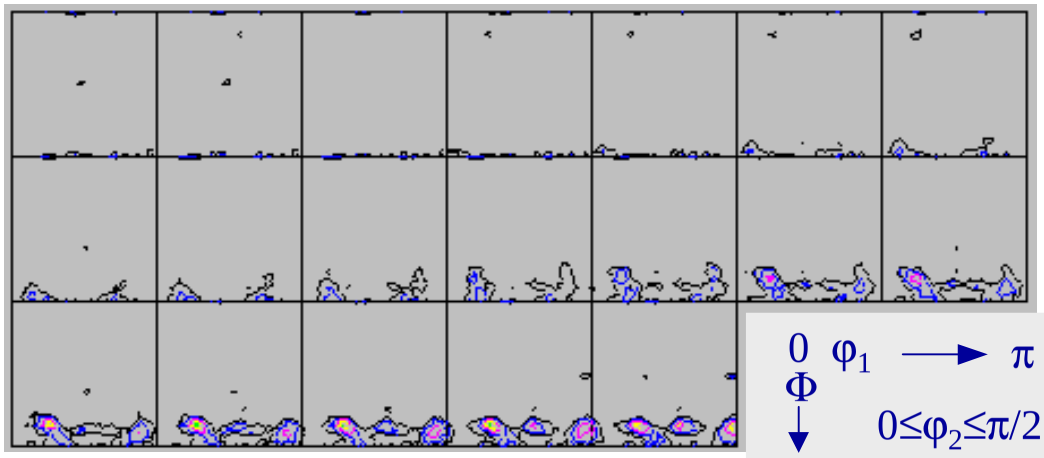

$0 \le \varphi_1 \le \pi$

Φ: $0 \rightarrow \pi$

$0 \le \varphi_2 \le \pi/2$

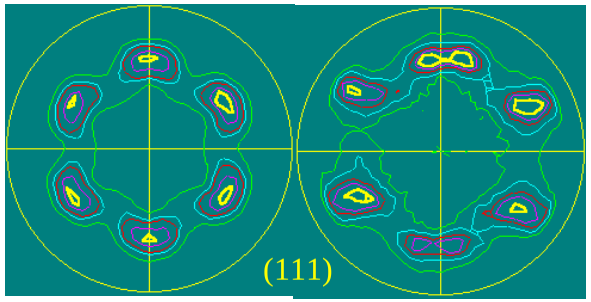

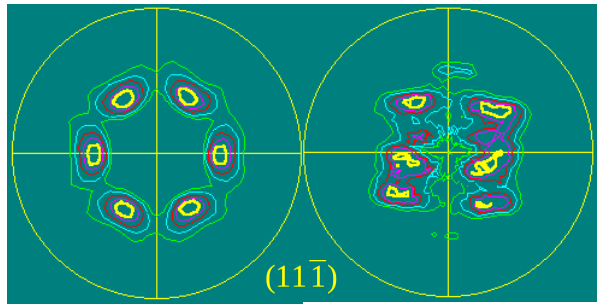

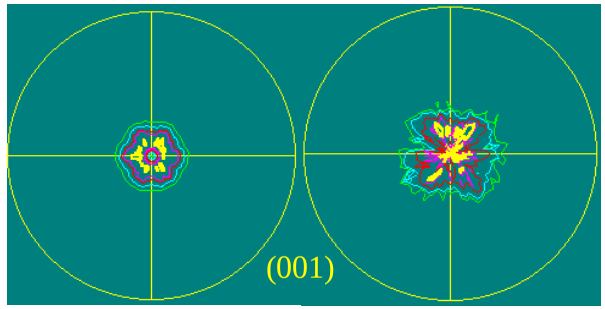

Application in Zr - ZrO_2 system

On LD sample

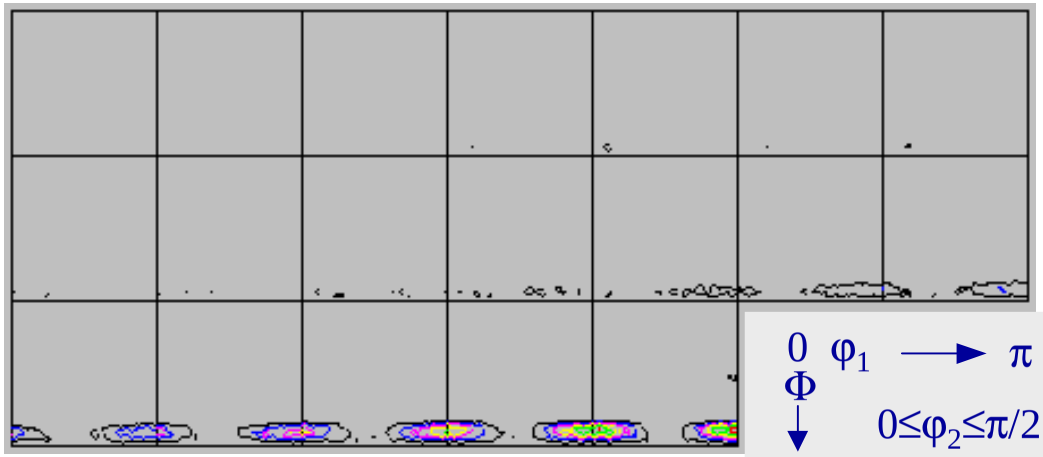

$0 \le \varphi_1 \le \pi$

Φ: $0 \rightarrow \pi$

$0 \le \varphi_2 \le \pi/2$

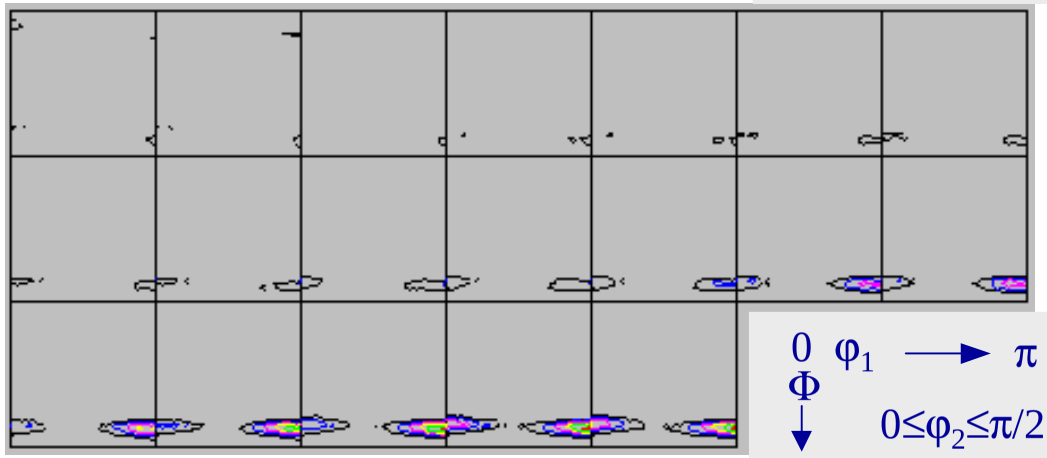

$0 \le \varphi_1 \le \pi$

Φ: $0 \rightarrow \pi$

$0 \le \varphi_2 \le \pi/2$

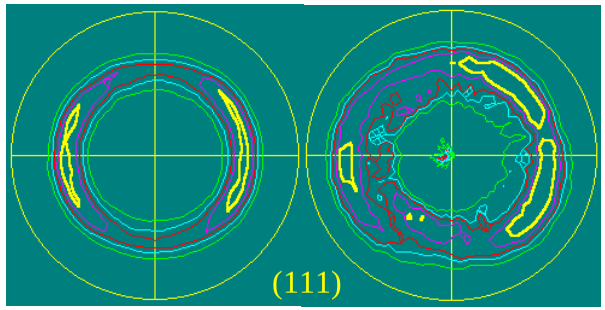

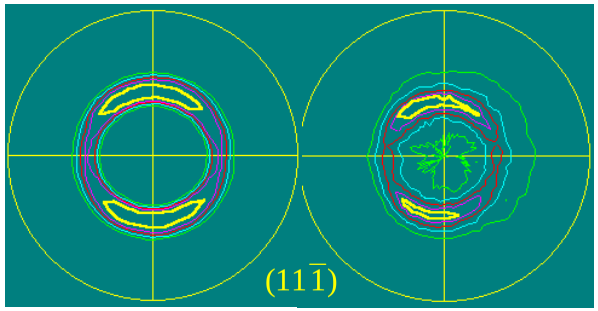

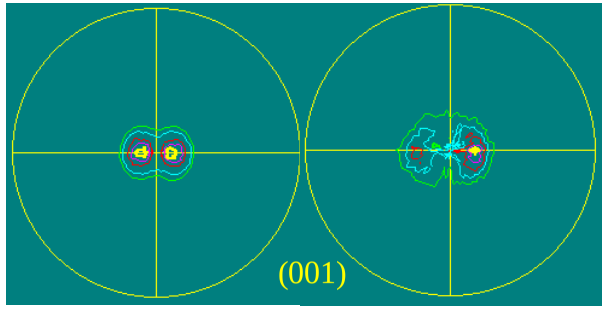

Contribution to the original knowledge

4) A mechanism of ZrO_2 texture and microstructure formation is proposed.

5) The diffusion mechanism in ZrO_2 is proposed.

6) The ODF of the oxide formed on the pressure tube is calculated for the first time.

7) A software is developed which can be used for the texture calculation in all the seven crystal systems

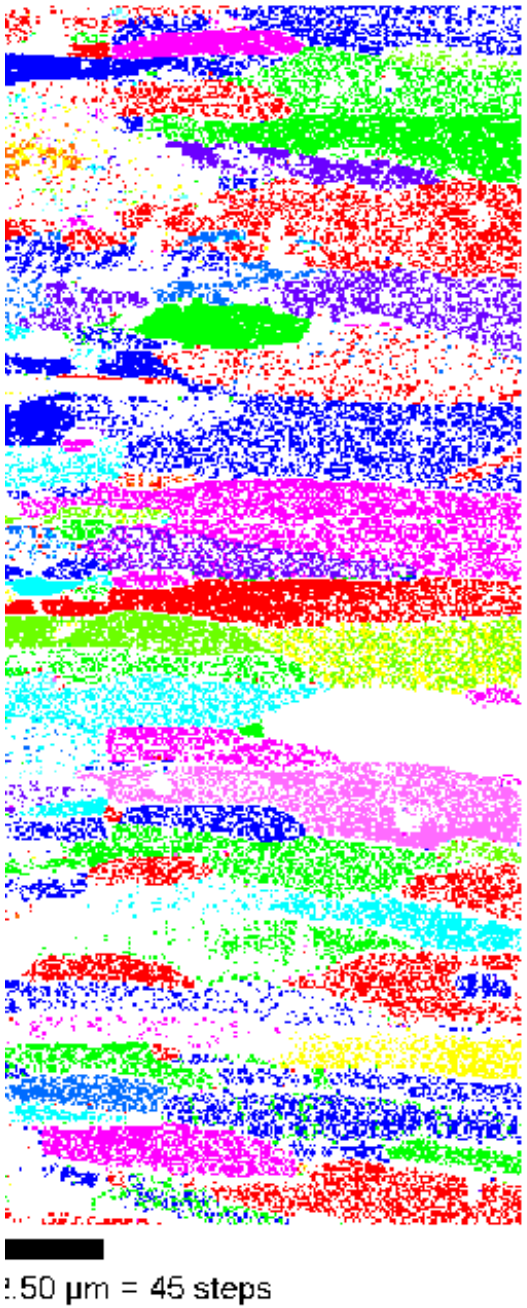

High Temperature Oxidation of Low Carbon Steel

Bae-Kyun Kim

Ph. D. Candidate

McGill

Dept. Mining and Metallurgical Eng. McGill University

Supervisor: Prof. J.A. Szpunar

Oxidation Mechanism

The assumptions of the model of diffusion-controlled oxidation:

- The isothermal heating process above 570 ′ .
- The isotropic oxide growth.

But, diffusion coefficient is one of anisotropic properties.

Industrial heat-treatment is a continuous heating.

Preliminary Results

(006) of Hematite

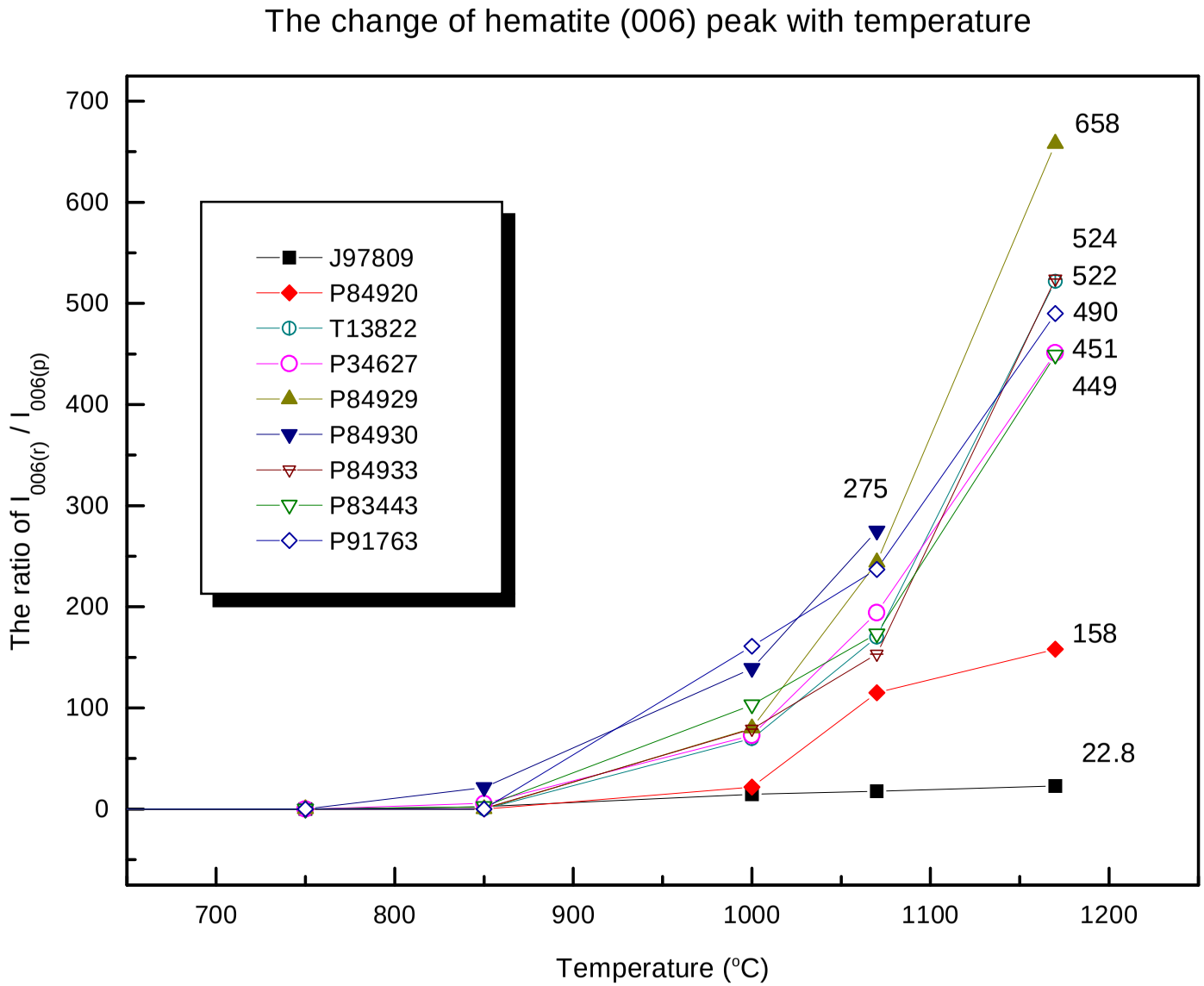

McGill

Preliminary Results

Microstructure of the oxides

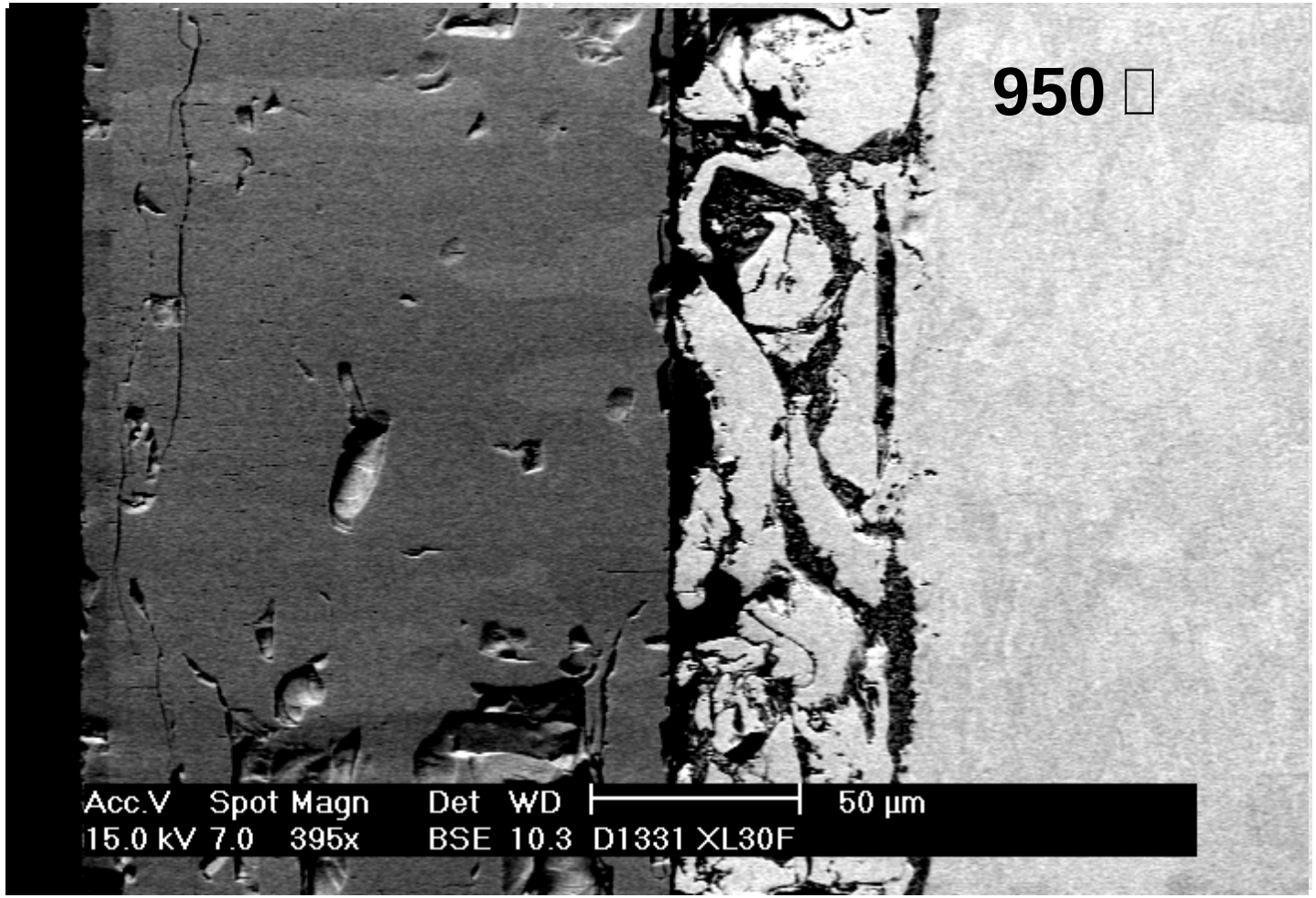

BSE image after dynamic oxidation of P83443 in the tube furnace.

McGill

Sputtering: Depiction of Energetic Particle Bombardment Effects on Surface and Growing Films.

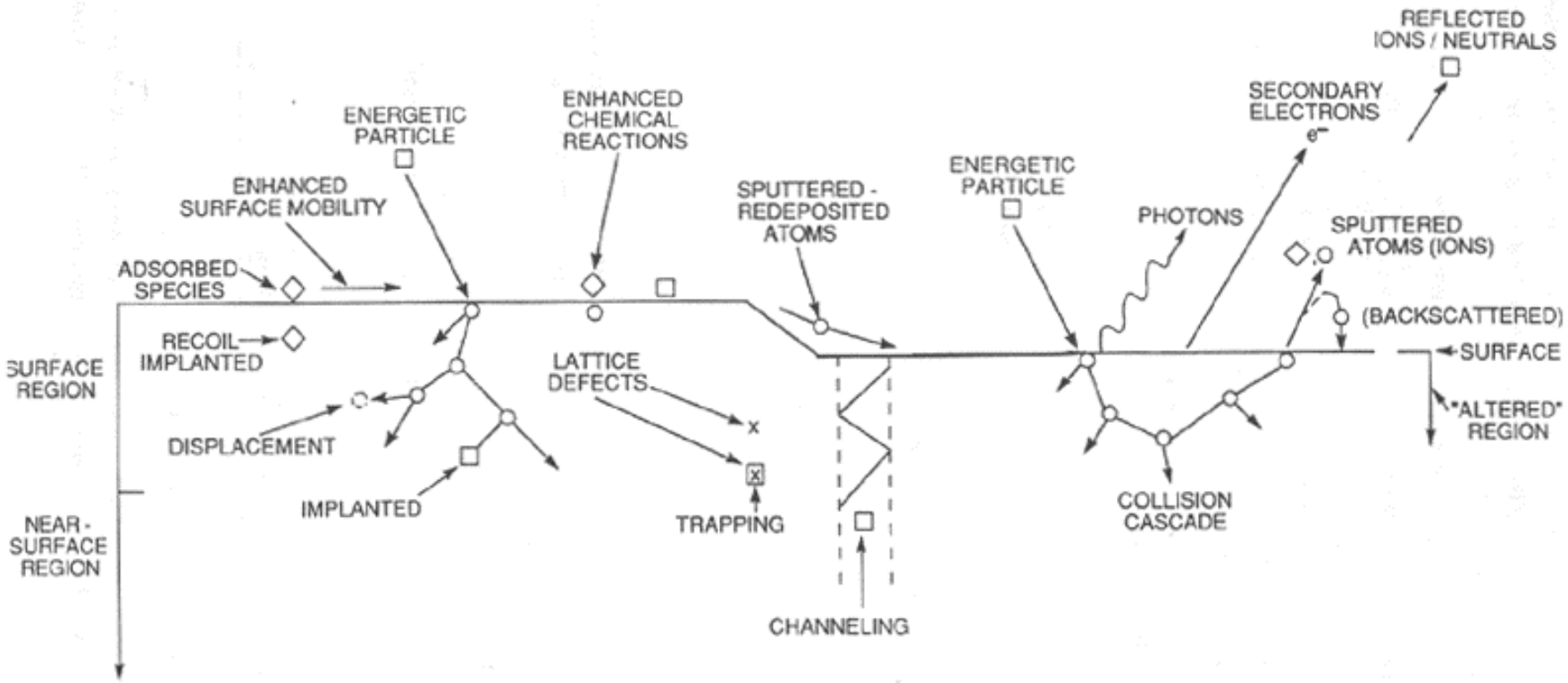

M. Ohring: The Materials Science of Thin Films

Texture and Electromigration Failure in Thin Films

* Electromigration
  — migration of the metal atoms along the metallic conductor carrying large current densities (current density in interconnects $\geq 4 \times 10^5$ A/cm^2)

* Damage (voids, hillocks) is formed by a depletion or accumulation of atoms.

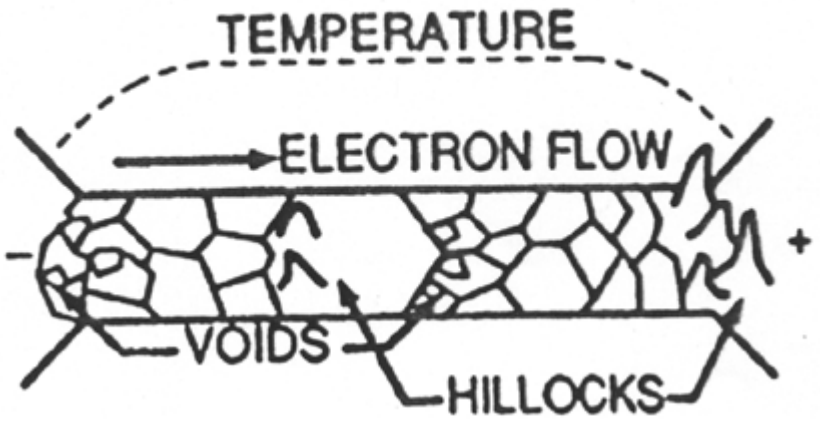

Table

Table 1
Constants used in the calculation of the influence of the texture on the magnetic properties

Legendre polynomials $\bar{P}_i(\alpha)$	Texture-susceptibility coefficient λ_i	Texture-remanence coefficient γ_i	Texture-coercivity coefficient δ_{Hi}	Texture-anisotropy field δ_{Ai}
$\bar{P}_0(\alpha)$	0.943	0.707	0.530	1.672
$\bar{P}_2(\alpha)$	-0.422	0.395	0.215	-0.145
$\bar{P}_4(\alpha)$	0	-0.088	-0.082	0.223
$\bar{P}_6(\alpha)$	0	0.040	0.077	-0.061
$\bar{P}_8(\alpha)$	0	-0.023	-0.011	0.032
$\bar{P}_{10}(\alpha)$	0	0.015	0.020	-0.035
$\bar{P}_{12}(\alpha)$	0	-0.010	-0.005	0.051
$\bar{P}_{14}(\alpha)$	0	0.008	0.013	-0.023
$\bar{P}_{16}(\alpha)$	0	-0.006	-0.002	0.033
$\bar{P}_{18}(\alpha)$	0	0.005	0.007	-0.017
$\bar{P}_{20}(\alpha)$	0	-0.004	-0.002	0.024

Schematic of Σ71b misorientation in monoclinic ZrO_2

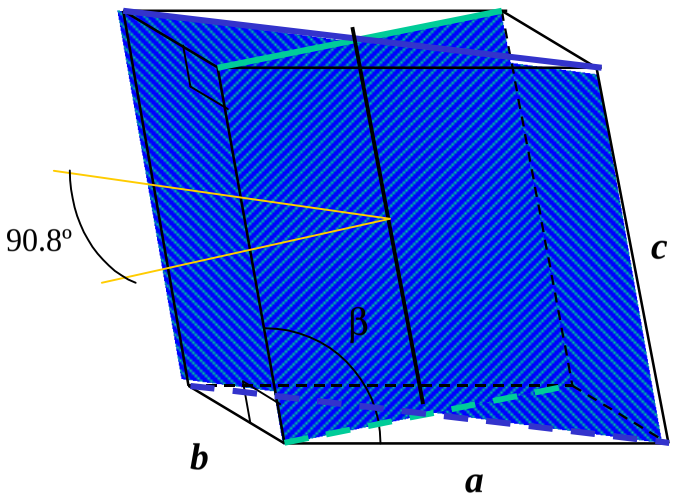

Formula for Texture Dependant Magnetic Properties

- Initial susceptibility

$$\chi = \frac{M^2}{2T}\sum_{l=0}^{L} t_l \lambda_l \quad ; T = \frac{1}{2}M^2(N_T - N_0) + K$$

- Remanence

$$\frac{M_R}{M_S} = \sum_{l=0}^{L} t_l \bar{\gamma}_l$$

- The coercive force

$$H_C = \frac{2T}{M}\sum_{l=0}^{L} t_l \delta_{Cl}$$

- The anisotropy field

$$H_A = \frac{4T}{M}\sum_{l=0}^{L} t_l \delta_{Al}$$

Comparison of the Measured and Calculated Coercivity

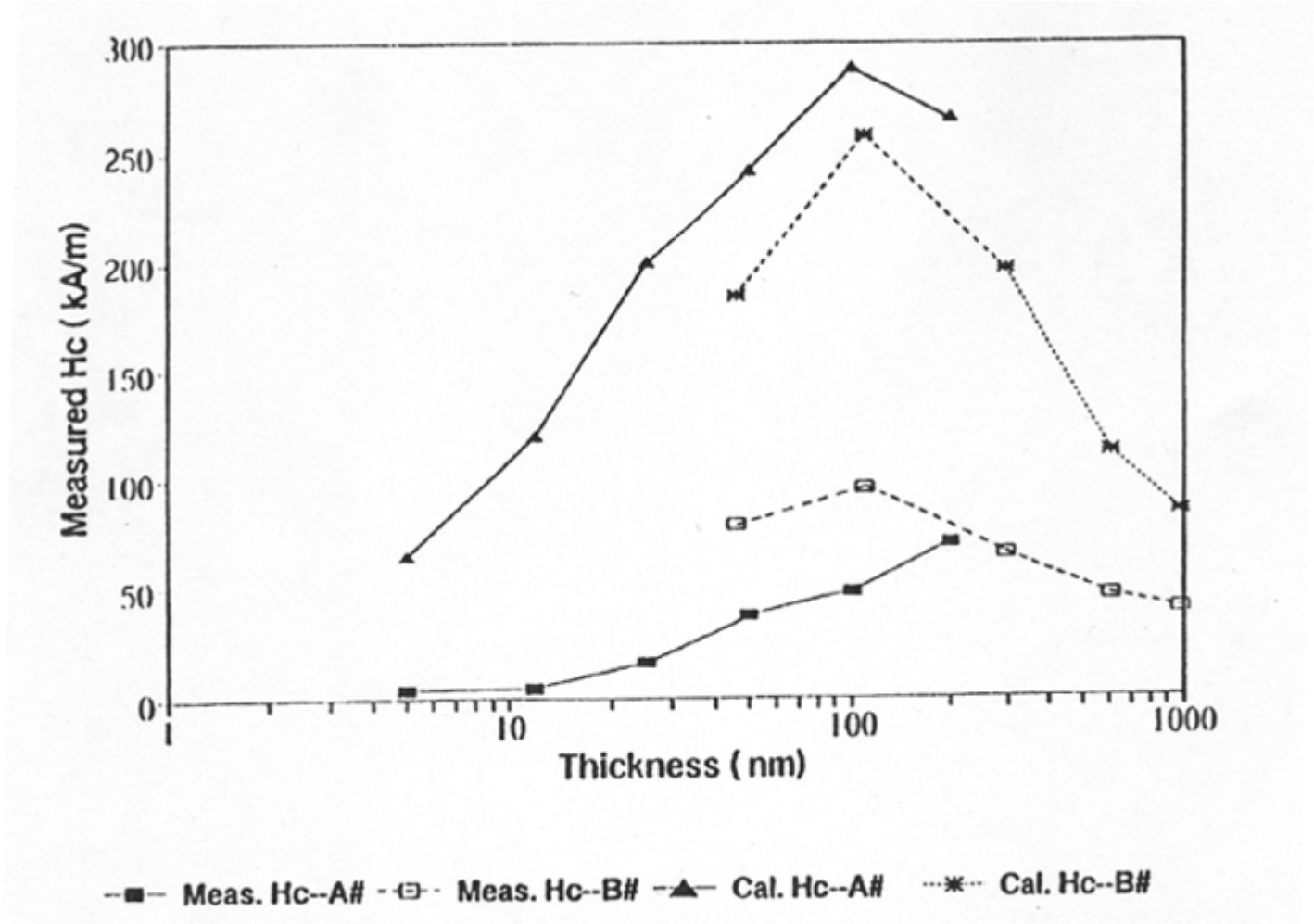

Application in Zr - ZrO_2 system

Selection of samples